Chaos Monte Carlo computation: a dynamical effect of random-number generations ¹

Ken Umeno

Communications Research Laboratory
Ministry of Posts and Telecommunications
4-2-1 Nukui-Kitamachi, Koganei, Tokyo 184-8795, Japan
(Received: December 11)

Abstract

Ergodic dynamical systems with absolutely continuous invariant probability measures are implemented as random-number generators for Monte Carlo computation. Such chaos-based Monte Carlo computation yields sometimes unexpected dynamical dependency behavior which cannot be explained by the usual statistical argument. We resolve the problem of its origin of this behavior by considering the effect of dynamical correlation on chaotic random-number generators. Furthermore, we find that superefficient Monte Carlo computation can be carried out by using chaotic dynamical systems as random-number generators. Here superefficiency means that the expectation value of the square of the error decreases to 0 in the order $\frac{1}{N^2}$ with N successive observations for $N \to \infty$, whereas the conventional Monte Carlo simulation gives the square of the error in the order $\frac{1}{N}$. The computation speed of the superefficient case does not depend on the dimensionality s of the problems and, hence, it is superior to the low-discrepancy sequences yielding the square of the error $\frac{(lnN)^{2s}}{N^2}$ in the known theoretical bounds. By deriving a necessary and sufficient condition for the superefficiency, it is shown that such high-performance Monte Carlo simulations can be carried out only if there exists a strong correlation of chaotic dynamical variables. Numerical calculation illustrates this dynamics dependency and the superefficiency of chaos Monte Carlo computations.

02.70.Lq 05.45.+b

 $^{^{1}}$ submitted to $Physical\ Review\ E$

1 Introduction

The applications of physical processes to efficient computation have been recently gaining an attention. Among many kinds of natural phenomena, chaos has a peculiar merit such that while the implementations of chaos are rather easy in computers or in some physical devices, it exhibits stochastic behavior as well as the deterministic nature. Thus, it is of great interest to investigate what kinds of efficient computations can be harnessed by chaos. Since chaotic phenomena are described by dynamical systems, the numbers generated by chaotic dynamical systems can be considered as pseudo-random numbers. So the right question must be focused on the distinguishable things between chaos and the conventional pseudo random-number generators to perform some computation. While various proposals of tests for qood random-number generators have been already extensively studied from the viewpoint of general aspects of random-number generations [1], such comparison studies between chaos and pseudo random-number generators have rarely been made. One exception is the study by Phatak and Rao, which showed that the logistic map passed some statistical tests that ideal i.i.d. (independently, identically distributed) random-number generators must pass [2]. In this paper, we study chaotic (ergodic) dynamical systems as special-purpose random-number generators for Monte Carlo methods, which are very powerful and general methods with many practical applications [3, 4].

From the beginning, the key issue of the Monte Carlo method has been the method of generating random numbers [5]. However, no efficient chaotic randomnumber generator which is superior to the conventional pseudo random-number generators in Monte Carlo simulations has yet reported. The main purpose of this paper is to show that superefficient Monte Carlo computation can be performed by utilizing dynamical correlation of chaotic dynamical systems. In this superefficient case, the expectation value of the square of the error in Monte Carlo simulations decreases to 0 in the order of $\frac{1}{N^2}$ with N successive observations for $N \to \infty$, while the corresponding value of the conventional Monte Carlo simulations decreases to 0 in the order of $\frac{1}{N}$ for $N \to \infty$. The convergence speed of superefficient Monte Carlo simulations is therefore greatly accelerated by making use of chaotic dynamical systems as random-number generators. Since any Monte Carlo computation can be formulated as a problem of evaluating an integral over a certain domain, here we consider the problem of Monte Carlo integration to elucidate the superefficiency of chaos-based Monte Carlo computation. We do this by analyzing how a local dynamical characteristic (thus, non-random nature) of chaotic random-number generators globally affects macroscopic (statistical) observable errors. The Monte Carlo method is essentially based on the ergodic principle: When random numbers $\{\xi_i\}_{i=1...}$ are uniformly distributed over Ω (thus ergodic with respect to the Lebesgue measure on Ω), the following identity holds according to the ergodic theorem (or equivalently according to the strong law of large numbers).

$$\int_{\Omega} f(x)dx = \lim_{N \to \infty} \frac{1}{N} \sum_{j=1}^{N} f(\xi_j). \tag{1}$$

A sum $\frac{1}{N}\sum_{j=1}^{N} f(\xi_j)$ can thus approximate the integral $\int_{\Omega} f(x)dx$ with an error in the order of $\frac{1}{\sqrt{N}}$ when N is a large number. In this paper, we combine this ergodic principle in Monte Carlo simulations with some ideas about generating nonuniform random numbers by ergodic dynamical systems [6, 7, 8, 9]. This paper is organized as follows. In Section 2, our Monte Carlo algorithm based on ergodic (chaotic) dynamical systems is explained. In Section 3, we demonstrate that phenomena of dynamical dependency of chaos-based Monte Carlo simulations are illustrated by a set of chaotic dynamical systems with unique invariant measures. In Section 4, we clarify the necessary and sufficient condition for achieving the superefficiency such that the proposed chaos-based Monte Carlo simulations are superior to conventional Monte Carlo Simulations. Section 5 presents numerical results of such superefficient chaos-based Monte Carlo simulations for a one-dimensional integration problem with integrands via Chebyshev-polynomial expansions. In Section 6, numerical results of superefficient chaos-based Monte Carlo simulations for a multi-dimensional integration problem are given. Section 7 presents numerical results of superefficient chaos-based Monte Carlo simulations for an integration problem over the infinite support $(-\infty,\infty)$. A physical meaning of these superefficient chaos Monte Carlo computations is given in Section 8. And a summary and discussion are given in Section 9.

2 Chaos-Based Monte Carlo Algorithm

Consider a dynamical system $X_{n+1} = F(X_n)$ which is ergodic with respect to an invariant probability measure $\rho(x)dx$ with $\rho(x)$ being a continuous density function $\rho: \Omega \to R$. This means that the measure $d\mu(x) = \rho(x)dx$ is invariant under time evolution and, furthermore, is absolutely continuous with respect to the Lebesgue measure on Ω . This dynamical system can thus be seen as a random-number generator with a sampling measure $\rho(x)dx$ on the domain Ω . In this case, according to the Birkhoff Ergodic Theorem [10], for any function A(x) satisfying

$$\int_{\Omega} |A(x)| dx < \infty, \tag{2}$$

the time average, $\lim_{N\to\infty} \frac{1}{N} \sum_{i=0}^{N-1} \frac{A(X_i)}{\rho(X_i)}$ is equal to the space average $\int_{\Omega} A(x) dx$ for almost every X_0 with respect to the probability measure $\rho(x) dx$ such that

$$\overline{A/\rho} = \langle A/\rho \rangle = \int_{\Omega} A(x)dx,$$
 (3)

where

$$\overline{B} \equiv \lim_{N \to \infty} \frac{1}{N} \sum_{i=0}^{N-1} B(X_i)$$
(4)

and

$$\langle B \rangle \equiv \int_{\Omega} B(x) \cdot \rho(x) dx.$$
 (5)

This means that the space average represented by $\int_{\Omega} A(x)dx$ can be computed by the time-average of successively generated observables $B_i \equiv B(X_i) = A(X_i)/\rho(X_i)$ by generated by this chaotic dynamical system. In the same way, we can obtain a Monte Carlo algorithm for multiple-dimensional integrals:

$$\overline{A/\rho_s} \equiv \lim_{N \to \infty} \frac{1}{N} \sum_{i=0}^{N-1} \frac{A(X_{1,i}, \dots, X_{n,i})}{\prod_{j=1}^s \rho(X_{j,i})} = \langle A/\rho_s \rangle = \int_{\Omega} A(x) dx, \tag{6}$$

where $\rho_s(x) = \prod_{i=1}^s \rho(x_i)$, $dx = \prod_{i=1}^s dx_i$, and $\langle B(x) \rangle = \int_\Omega B(x) \rho_s(x) dx$. Here, we assume that each dynamics $X_{j,i+1} = F_j(X_{j,i})$ has the same invariant probability measure $\rho(x)dx$. Thus, any ergodic dynamical systems with respect to an explicit invariant probability measures $\rho(x)dx$, in principle, can serve as random-number generators for Monte Carlo simulations in calculating arbitrary multiple integrals. However, such dynamical Monte Carlo computation cannot be carried out unless their invariant densities $\rho(x)$ are explicitly known. In recent years, many chaotic dynamical systems have been derived, which have explicit invariant measures with continuous densities [8, 9]. Hence these chaotic dynamical systems can offer their applications for use as random-number generators for Monte Carlo simulations. Clearly, these random-number generators using chaos have strict time-correlation which is not desirable for ideal random-number generators. Suppose N successive observations, $A_i \equiv A(X_i)$, $\rho_i \equiv \rho(X_i)$, $i = 1, \dots, N$, of quantities A(x) and a density function $\rho(x)$ have been stored. We consider the expectation value of the square of the error as

$$\sigma(N) \equiv \langle \langle \left[\frac{1}{N} \sum_{i=0}^{N-1} A_i / \rho_i - \langle A/\rho \rangle \right]^2 \rangle \rangle, \tag{7}$$

where the expectation of B denoted by $\langle \langle B \rangle \rangle$ means an ensemble average with respect to the initial conditions X_0 with a sampling measure $\rho(x)dx$. As proved in Appendix A, this expectation value $\sigma(N)$ is given by the two-point correlation functions of $B_i = B(X_i)$ as follows:

$$\sigma(N) = \frac{1}{N} \{ \langle B^2 \rangle - \langle B \rangle^2 \} + \frac{2}{N} \sum_{j=1}^{N} (1 - \frac{j}{N}) \{ \langle B_0 B_j \rangle - \langle B \rangle^2 \}, \tag{8}$$

where $B(x) \equiv A(x)/\rho(x)$. From Eq. (8), we can see that $\sigma(N)$ is composed of the statistical variance term

$$\sigma_s(N) \equiv \frac{1}{N} \{ \langle B^2 \rangle - \langle B \rangle^2 \}, \tag{9}$$

which purely depends on the form of the integrand B and the dynamical correlation term

$$\sigma_d(N) \equiv \frac{2}{N} \sum_{j=1}^{N} (1 - \frac{j}{N}) \{ \langle B_0 B_j \rangle - \langle B \rangle^2 \}, \tag{10}$$

which depends on the chaotic dynamical systems $X_{n+1} = F(X_n)$ utilized as random-number generators. From the above formula, when there exists a negative covariance (correlation) term such that

$$\sum_{j=1}^{N} \{ \langle B_0 B_j \rangle - \langle B \rangle^2 \} < 0, \tag{11}$$

the total variance can be reduced. So such negative correlated variables (antithetic variables) have been used as a variance reduction technique in the Monte Carlo method[11]. In the next section, we consider such a dynamical correlation term of chaotic random-number generators in detail.

3 Dynamical Dependency

To test the dynamical correlation effect in chaotic random-number generators, we investigate chaos-based Monte Carlo computations of simple integration problems on the unit interval $\Omega = [0,1]$ by using chaotic dynamical systems with the same statistics described by a unique invariant measure. Chaotic dynamical systems utilized as random-number generators here are listed in Table 1. In all of the numerical computations in this paper, we use M(=1000) different initial conditions $X_0(j)$ for $j = 1, \dots, M$. We measure the numerical values of an empirical average of the square of the error defined by

$$V(N) = \frac{1}{M} \sum_{i=1}^{M} \left[\frac{1}{N} \sum_{i=0}^{N-1} A_i(j) / \rho_i(j) - \langle A/\rho \rangle \right]^2.$$
 (12)

Since the numerical sampling does not obey the probability measure $\rho(x)dx$ exactly, the observed value V(N) is not equal to the exact ensemble average of the square of the error $\sigma(N)$ but fluctuates around $\sigma(N)$. However, we can expect that

$$V(N) \to \sigma(N) \quad M \to \infty$$
 (13)

because the central limit theorem holds for random variables

$$v_j \equiv \left[\frac{1}{N} \sum_{i=0}^{N-1} A_i(j) / \rho_i(j) - \langle A/\rho \rangle\right]^2, \quad j = 1, \dots, M$$
 (14)

for $M\to\infty$. Thus, the simulation results here does not depend on the precise sampling information of the initial data $\{X_0(j)\}_{j=1,\cdots,M}$. Figure 1 shows that although Ulam-von Neumann map, Cubic map and Quintic map have the same invariant measure $\rho(x)dx=\frac{dx}{\sqrt{x(1-x)}}$, the resulting error variances of chaosbased Monte Carlo integration of $I=\int_0^1 x^3 dx=\frac{1}{4}$ exhibit discrepancy between them. Similar results hold for the generalized Ulam-von Neumann map and generalized Cubic map, both of which have the same invariant measure $\rho(x)dx=\frac{dx}{\sqrt{x(1-x)(1-\frac{1}{2}x)(1-\frac{3}{10}x)}}$. Figure 2 shows that there exists a significant

dynamical dependency of the expectation value of the square of the errors for chaos-based Monte Carlo integration of $I = \int_0^1 x(1-x)dx = \frac{1}{6}$ by using the same family of chaotic dynamical systems as of Fig.1. Furthermore, these figures show that the chaotic random-number generator resulting in the most efficient computation depends on the integrand (the generalized Cubic map for Fig. 1 and Ulam-von Neumann map for Fig. 2). Therefore, it is clear that these numerical results of chaotic random-number generators cannot be explained by the usual statistical argument such as the importance sampling. Hence, we must consider the dynamical effect of these chaotic random-number generators to explain these dynamical dependency phenomena. In the next section, we consider a extreme case of dynamical dependency resulting in superefficient chaos-based Monte Carlo simulations.

4 Condition for Superefficiency

Here, we derive the condition for attaining the superefficiency of chaos-based Monte Carlo simulations such that the expectation value of the square of the error decreases to 0 in the order of $\frac{1}{N^2}$ for $N \to \infty$. As mentioned in Section 2, if random variables generated by chaotic random-number generators have a negative correlation, the resulting expectation value $\sigma(N)$ of the square of the error can be reduced as the usual variance reduction technique. Furthermore, we have a stronger statement in the case that a chaotic dynamical system has a mixing (thus, ergodic) property as follows:

Theorem 1 (Superefficiency Condition) The expectation value of the square of the error $\sigma(N)$ decreases to zero in the order of $\frac{1}{N^2}$ as

$$\sigma(N) = -\frac{2}{N^2} \sum_{j=1}^{N} j \{ \langle B_0 B_j \rangle - \langle B \rangle^2 \} = O(\frac{1}{N^2}) \to 0 \quad \text{for} \quad N \to \infty, \tag{15}$$

if and only if the relation

$$\langle B^2 \rangle - \langle B \rangle^2 + 2 \sum_{j=1}^{\infty} \{ \langle B_0 B_j \rangle - \langle B \rangle^2 \} = 0$$
 (16)

is satisfied.

The proof of the theorem is given as follows. Since $\sigma(N)$ has the following identity from formula (8):

$$\sigma(N) = \frac{\langle B^2 \rangle - \langle B \rangle^2 + 2\sum_{j=1}^N \{\langle B_0 B_j \rangle - \langle B \rangle^2\}}{N} - \frac{2}{N^2} \sum_{j=1}^N j \{\langle B_0 B_j \rangle - \langle B \rangle^2\},\tag{17}$$

we have the relation

$$\sigma(N) = O(\frac{1}{N^2}) \quad \text{for} \quad N \to \infty \iff \langle B^2 \rangle - \langle B \rangle^2 + 2 \sum_{j=1}^{\infty} \{ \langle B_0 B_j \rangle - \langle B \rangle^2 \} = 0.$$
(18)

According to the mixing property of the chaotic dynamical systems with Lyapunov exponents $\lambda(>0)$, we have

$$\langle B_0 B_j \rangle - \langle B \rangle^2 = O[e^{-j\lambda}] \to 0, \quad \text{for} \quad j \to \infty,$$
 (19)

which assures the convergence of the infinite sums $\sum_{j=1}^{\infty} \{\langle B_0 B_j \rangle - \langle B \rangle^2\}$ and $\sum_{j=1}^{\infty} j \{\langle B_0 B_j \rangle - \langle B \rangle^2\}$ in the superefficiency condition (16). It is clear that Theorem 1 gives us a necessary and sufficient condition for the superefficiency of the chaos-based Monte Carlo simulations. Furthermore, Theorem 1 about the condition for superefficiency does not depend on the dimensionality s of integration domains. Thus, we call the condition given in Eq.(16) the superefficiency condition for general s-dimensional Monte Carlo integration problems.

The superefficiency here is reminiscent of low-discrepancy sequences (or quasirandom numbers) generated by a deterministic algorithm, where the theoretical error bounds are known to be of size $O\left[\frac{(\ln N)^s}{N}\right]$ for s-dimensional integration problems, which are also superior to the conventional Monte Carlo simulations with the error of size $O(\frac{1}{\sqrt{N}})$ [12]. Consequently, the theoretical values of the square of the error in the low-discrepancy sequences are in the order of $O\left[\frac{(\ln N)^{2s}}{N^2}\right]$. Thus, a particular superefficient Monte Caro simulation using chaos is superior to lowdiscrepancy sequences in the sense that the expected value $\sigma(N)$ of the square of the error in the superefficient Monte Carlo simulation is $O(\frac{1}{N^2})$ where the logarithmic factor $(\ln N)^{2s}$, which is not negligible for a large dimensionality s, is removed from the corresponding order of the low-discrepancy sequences. Table 2 compares the data about the order of the square of the errors. Besides the differences in the order, the following differences between the two deterministic methods of Monte Carlo computations exist. While it is difficult for explicitly estimating the error for low-discrepancy sequences, this superefficient Monte Carlo computations can give an exact estimate of the mean error variance as in Eq. (16). However, the present superefficient chaos-based Monte Carlo computations, which are superior to low-discrepancy sequences in higher dimension s, can be carried out only if there exists a negative correlation of chaotic dynamical variables satisfying superefficiency condition (16). In the following sections, we will present concrete examples yielding superefficient chaos Monte Carlo computations.

5 Superefficiency: A Case of Chebyshev Maps

Here, we achieve superefficiency $\sigma(N) = O(\frac{1}{N^2})$ for a certain family of onedimensional integration problems by using a set of specific chaotic dynamical systems $X_{n+1} = T_p(X_n)$, where $T_p(X)$ is the *p*-th order Chebyshev polynomial defined by $T_p[\cos(\theta)] \equiv \cos(p\theta)$ at $p \geq 2$. Examples of Chebyshev polynomials are given by

$$T_0(X) = 1, T_1(X) = X, T_2(X) = 2X^2 - 1, T_3(X) = 4X^3 - 3X, \cdots$$
 (20)

It is known [7] that these Chebyshev maps T_p are mixing (thus, ergodic) with respect to the invariant measure $\frac{dx}{\pi\sqrt{1-x^2}}$ on the domain $\Omega=[-1,1]$ for $p\geq 2$ and they have Lyapunov exponents $\ln p$. Note that the chaotic dynamical system $X_{n+1}=T_2(X_n)=2X_n^2-1$ is equivalent to the well-known logistic dynamical system $Y_{n+1}=4Y_n(1-Y_n)$ with an invariant measure $\frac{dy}{\pi\sqrt{y(1-y)}}$ on the unit interval [0,1][6]. In the same way, chaotic dynamics caused by the third-order Chebyshev map $X_{n+1}=T_3(X_n)=4X_n^3-3X_n$ is equivalent to the cubic chaos $Y_{n+1}=Y_n(3-4Y_n)^2$ with Lyapunov exponent $\ln 3$. It is also known that a system of Chebyshev polynomials constitutes a complete orthonormal system satisfying the relations

$$\int_{-1}^{1} T_i(x) T_j(x) \rho(x) dx = \delta_{i,j} \frac{(1 + \delta_{i,0})}{2}, \tag{21}$$

where $\delta_{i,j}$ stands for the Kronecker delta function such that

$$\delta_{i,j} = \begin{cases} 1 & i = j \\ 0 & i \neq j. \end{cases}$$
 (22)

Consider a one-dimensional continuous function B(x) as an integrand on the domain $\Omega = [-1, 1]$. By Weierstrass's approximation theorem, for an arbitrary $\epsilon > 0$, there exists a polynomial function P(x) satisfying

$$|B(x) - P(x)| < \epsilon$$
 for $-1 \le x \le 1$.

We can thus uniquely expand an arbitrary integrand (continuous function) B(x) in terms of Chebyshev polynomials (orthogonal-basis functions):

$$B(x) = \sum_{k=0}^{\infty} b_k T_k(x) = \sum_{k=0}^{\infty} \frac{2}{1 + \delta_{k,0}} \langle BT_k \rangle T_k(x),$$

where the coefficients are given by the formula

$$b_k = \frac{2}{(1 + \delta_{k,0})} \int_{-1}^1 B(x) T_k \rho(x) dx = \frac{2}{1 + \delta_{k,0}} \langle BT_k \rangle.$$

The completeness of the system of Chebyshev orthogonal functions assures that

$$b_k \to 0 \quad \text{for} \quad k \to \infty.$$
 (23)

Thus, it can be said that any continuous function can be well approximated in terms of finite numbers of Chebyshev polynomials. So we consider the Monte Carlo integration problem of an integrand

$$B(x) = \sum_{k=0}^{L} b_k T_k(x).$$
 (24)

Since

$$B[T_j(x)] = \sum_{k=0}^{L} b_k T_k [T_j(x)] = \sum_{k=0}^{L} b_k T_{kj}(x),$$
 (25)

we can calculate two-point correlation functions $\langle B_0 B_j \rangle (= \langle B(x) B[T_{p^j}(x)] \rangle)$ computed by the p-th Chebyshev map T_p as follows:

$$\langle B_0 B_j \rangle = \langle b_0 + \sum_{k=1}^{L} b_k T_k(x), b_0 + \sum_{k=1}^{L} b_k T_{k \cdot p^j}(x) \rangle$$

$$= \begin{cases} b_0^2 + \frac{1}{2} \sum_{k=1}^{[L/p^j]} b_{kp^j} b_k & j \leq [\log_p L] \\ b_0^2 & j \geq [\log_p L] + 1 \end{cases}$$
(26)

where [x] is the largest non-negative integer part of x. It can be seen from Eq. (26) that when p > L, the p-th Chebyshev map causes no dynamical effect such that $\sigma(N) = \sigma_s(N)$. Hence from now on, we consider the case $p \leq L$. The statistical variance term is given by

$$\sigma_s(N) = \frac{1}{N} \{ \langle B^2 \rangle - \langle B \rangle^2 \} = \frac{1}{2N} (\sum_{m=1}^L b_m^2),$$
 (27)

and the dynamical correlation term of the variance of error is given by

$$\sigma_d(N) = \frac{2}{N} \sum_{j=1}^{N} (1 - \frac{j}{N}) \{ \langle B_0 B_j \rangle - \langle B \rangle^2 \} = \frac{2}{N} \sum_{j=1}^{\lceil \log_p L \rceil} \{ (1 - \frac{j}{N}) \} \sum_{m=1}^{\lceil L/p^j \rceil} b_{mp^j} b_m.$$
 (28)

The condition for the superefficiency in Eq. (16) is thus given in terms of the coefficients of the Chebyshev expansions of an integrand $B(x) = \sum_{m=0}^{L} b_m T_m(x)$ as follows:

$$\sum_{j=1}^{\infty} \{ \langle B_0 B_j \rangle - \langle B \rangle^2 \} = \sum_{j=1}^{\lfloor \log_p L \rfloor} \sum_{m=1}^{\lfloor L/p^j \rfloor} b_{mp^j} b_m = -\frac{1}{2} (\sum_{m=1}^{L} b_m^2) < 0, \tag{29}$$

where the Monte Carlo simulations are computed by the p-th Chebyshev map T_p . Therefore, for any integrand given by Chebyshev expansions as Eq. (24), a dynamical correlation term represented by the L.H.S. of Eq. (29) must thus be negative to satisfy the superefficiency condition As is clearly seen in Eq. (29), the constant term b_0 is irrelevant for the superefficiency. Here we can give a family of examples that meet the superefficiency condition as follows.

Consider the case that a normalized integrand $B(x) = \frac{A(x)}{\rho(x)}$ has the following form

$$B(x) = a_c + \sum_{m=0}^{L} a_m T_{p^m}(x) = \frac{A(x)}{\rho(x)},$$
(30)

where $p \geq 2$. Note that

$$\langle B \rangle = a_c \quad \text{and} \quad \langle B^2 \rangle = a_c^2 + \frac{1}{2} \sum_{m=0}^{L} a_m^2.$$
 (31)

In this case, the following two-point correlation functions are simply given by

$$\langle B_0 B_l \rangle = \langle a_c + \sum_{m=0}^{L} a_m T_{p^m}(x), a_c + \sum_{m=0}^{L} a_m T_{p^{m+l}}(x) \rangle = a_c^2 + \frac{1}{2} \sum_{m=l}^{L} a_m a_{m-l}, \quad (32)$$

Thus, with the use of formula (8), the expectation value of the square of the error $\sigma(N)$ is explicitly given by the following formula:

$$\sigma(N) = \frac{1}{2N} \left(\sum_{m=0}^{L} a_m\right)^2 - \frac{1}{N^2} \sum_{l=1}^{L} \sum_{m=l}^{L} l a_m a_{m-l}.$$
 (33)

Therefore, superefficiency condition (16) is equivalent to the simple condition

$$\sum_{m=0}^{L} a_m = 0. (34)$$

In other words, when condition (34) is satisfied, the O(1/N) term of $\sigma(N)$ can be eliminated. Hence, if an integrand has a form of Eq. (30) with the condition $\sum_{m=0}^{L} a_m = 0$, the superefficient Monte Carlo computation can be carried out by the p-th order Chebyshev chaos map such that the resulting expectation value of the square of the error are given as follows:

$$\sigma(N) = -\frac{1}{N^2} \sum_{l=1}^{L} \sum_{m=l}^{L} l a_m a_{m-l} = O(\frac{1}{N^2}).$$
 (35)

On the other hand, even if an integrand satisfies the above condition, other types of chaotic dynamics, such as, $X_{j+1} = T_{p'}(X_j)$ for $p' \neq p$ then cause the time-correlation functions to exhibit no dynamical effect:

$$\langle B_0 B_l \rangle = \langle a_c + \sum_{m=0}^{L} a_m T_{p^m}(x), a_c + \sum_{m=0}^{L} a_m T_{p^m \cdot p'^l}(x) \rangle = a_c^2 = \langle B \rangle^2.$$
 (36)

Therefore, $\sigma(N)$ in this case does not so quickly decrease to 0 for $N \to \infty$ as the superefficient cases but normally converges to 0:

$$\sigma(N) = \sigma_s(N) = \frac{1}{2N} (\sum_{m=0}^{L} a_m^2) = O(\frac{1}{N}).$$
 (37)

This means that specific chaotic (Chebyshev) dynamical systems do exist in all of the Chebyshev chaotic dynamical systems, which make Monte Carlo computation superefficient and this selection of the Chebyshev chaotic dynamical systems for the superefficiency depends on a form of integrand, irrespective of the fact that all of the Chebyshev chaotic dynamical systems has the same invariant probability measure (the same statistics). It can thus be said that the superefficiency of chaos-based Monte Carlo simulations is caused not by a statistical effect but by a purely dynamical effect (thus, a non-random effect) with a strong correlation

of chaotic variables in random-number generators. To numerically confirm the interplay between an integrand and chaotic dynamical systems chosen as random-number generators, we consider a simple integrand on $\Omega = [-1, 1]$ as follows:

$$A(x) = \frac{x - 2x^2 + 1}{\pi\sqrt{1 - x^2}} = [T_1(x) - T_2(x)]\rho(x) = B(x)\rho(x).$$
 (38)

Here, this integrand corresponds to the case that $a_0 = 1$, $a_1 = -1$, L = 1, and p = 2 in Eq. (30), which clearly satisfies the above condition of superefficiency.

Thus, the random numbers generated by the second-order Chebyshev maps $X_{n+1} = T_2(X_n)$ are predicted to yield the expectation value of the square of the error,

$$V_{T_2}(N) \approx \sigma_{T_2}(N) = \frac{1}{N^2}$$
 (39)

by the formula (33), while the other types of the p-th Chebyshev maps at $p \geq 3$ are predicted to give the expectation value of square of error in the order of

$$V_{T_p}(N) \approx \sigma_{T_p}(N) = \frac{1}{N} \quad \text{for} \quad p > 2.$$
 (40)

Figure 2 shows that numerical results coincide with our prediction about the occurrence of the superefficiency of chaos-based Monte Carlo simulations. The superefficiency achieved here remarkably contrasts with the conventional Monte Carlo simulations with $V(N) \approx \sigma(N) = O(\frac{1}{N})$ computed by the other p-th Chebyshev maps p > 2. If p in Eq. (30) is a composite number such as $p = p'^k$ for an integer $k \geq 2$, the p'-th order Chebyshev map $T_{p'}$ also gives a superefficiency. To check this numerically, we consider an integrand

$$A(x) = [T_1(x) - T_4(x)]\rho(x) = \frac{(-8x^4 + 8x^2 + x - 1)}{\pi\sqrt{1 - x^2}}.$$

In this case, both the second-order Chebyshev map T_2 and the fourth-order Chebyshev map T_4 are predicted to give superefficient results such as

$$V_{T_2}(N) \approx \sigma_{T_2}(N) = \frac{2}{N^2} \tag{41}$$

and

$$V_{T_4}(N) \approx \sigma_{T_4}(N) = \frac{1}{N^2} \tag{42}$$

respectively, while the third-order Chebyshev map T_3 and the fifth-order Chebyshev map T_5 are predicted to give the normal behavior of the expectation value of the square of the error

$$V_{T_p}(N) \approx \sigma_{T_p}(N) = \frac{1}{N} \quad \text{for} \quad p = 3, 5.$$
 (43)

Figure 3 confirms that numerical data coincide with our prediction about the selection of chaotic dynamical systems for performing superefficient chaos-based

Monte Carlo computations. The sampling dependency of superefficiency were also numerically tested. Figure 4(a) shows the numerically obtained error variance V(N) coincides well with the exact mean value of the square of the error $\sigma(N)$ in Eq. (35) for the superefficient Monte Carlo computation of an $B(x) = T_1 - T_4 + T_0$ with the sampling measure well approximated by the invariant measure $\rho(x)$. Figure 4(b) shows that while there exists discrepancy between the numerical value and the exact value of the mean square of the error for the same problem with uniform sampling measure of initial data, the same kinds of superefficient Monte Carlo simulations are carried out. Thus, superefficient chaos-based Monte Carlo computation is very robust under our choice of the initial conditions of chaotic dynamical systems.

6 Superefficiency: A Case of Multi-Dimensional Integration

As for the case of one-dimensional Monte Carlo integration problems, we try to achieve the same superefficiency in the multi-dimensional integration problem. Let us consider the domain of integration as the s-dimensional cubic $\Omega_s = [-1, 1]^s$. Even in this multi-dimensional case, there exists the multi-dimensional version of Weierstrass's approximation theorem [13] which guarantees that for an arbitrary ϵ , there exists a polynomial function $P(x) = P(x_1, \dots, x_s)$ such that

$$|B(x) - P(x)| < \epsilon \quad \text{for} \quad x \in \Omega_s,$$
 (44)

where $B(x) = B(x_1, \dots, x_s)$ is a continuous function over the domain Ω_s . From the complete orthonormal property of the Chebyshev polynomials $\{T_l(x)\}$, we can construct $T_{j_1}(x_1)\cdots T_{j_s}(x_s)$ as an element the complete orthonormal basis functions spanning the functional space $\mathcal{L}^2(\Omega_s, \rho_s)$ such that

$$\mathcal{L}^{2}(\Omega_{s}, \rho_{s}) = \{B(x_{1}, \cdots, x_{s}) | \int_{\Omega_{s}} |B(x_{1}, \cdots, x_{s})|^{2} dx_{1} \cdots dx_{s} < \infty\}.$$
 (45)

Any continuous function $B(x_1, \dots, x_n) \in \mathcal{L}^2(\Omega_s, \rho_s)$ can thus be uniquely expanded in terms of the products of the Chebyshev polynomials as follows:

$$B(x_1, \dots, x_s) = \sum_{j_1, \dots, j_s > 0} b_{j_1, \dots, j_s} T_{j_1}(x_1) \dots T_{j_s}(x_s).$$
 (46)

Therefore, as is the one-dimensional case, superefficiency condition are given for any continuous function $B(x_1, \dots, x_n) \in \mathcal{L}^2(\Omega_s, \rho_s)$ in terms of coefficients of the Chebyshev expansions. Here, to present multi-dimensional superefficiency, we consider a more specific family of integrands with the form,

$$\frac{A(x)}{\rho_s(x)} = B(x) = B(x_1, \dots, x_s) = a_c + \sum_{m=0}^{L} a_m T_{p_1^m}(x_1) \dots T_{p_s^m}(x_s), \tag{47}$$

where each dynamical variable $X_{i,j}$ associated with x_i is computed by the $p_i(\geq 2)$ -th order Chebyshev map as $X_{i,j+1} = T_{p_i}(X_{i,j})$. Note that a polynomial $T(x_1, \dots, x_n) = T_{p_1^{m_1}}(x_1) \dots T_{p_s^{m_s}}(x_s)$ for $p_i \geq 0, m_i \geq 0$ is also an element of orthonormal basis-functions which constitutes a complete orthonormal system in the s-dimensional functional space $\mathcal{L}^2(\Omega_s, \rho_s)$. As in the one-dimensional case, by using the orthonormal property of the Chebyshev polynomials, we can compute the following two-point correlation functions:

$$\langle B_0 B_l \rangle = a_c^2 + \frac{1}{2^s} \sum_{m=l}^L a_m a_{m-l}.$$
 (48)

As will be proven in Appendix B, the expectation value of the square of the error $\sigma(N)$ is thus given by

$$\sigma(N) = \frac{1}{2^{s}N} \left(\sum_{m=0}^{L} a_{m}\right)^{2} - \frac{1}{2^{s-1}N^{2}} \sum_{l=1}^{L} \sum_{m=l}^{L} l a_{m} a_{m-l}.$$
 (49)

Therefore, if an integrand satisfies the superefficiency condition $\sum_{m=0}^{L} a_m = 0$, which is equivalent to the relation (16), s chaotic dynamical systems $X_{i,j+1} = T_{p_i}(X_{i,j})$ for $i = 1, \dots, s$ again yield a superefficient Monte Carlo computation with the expectation value of the square of error in the order of $\frac{1}{N^2}$ as follows:

$$\sigma(N) = -\frac{1}{2^{s-1}N^2} \sum_{l=1}^{L} \sum_{m=l}^{L} l a_m a_{m-l} = O(\frac{1}{N^2}).$$
 (50)

Thus, the superefficiency of chaos-based Monte Carlo computation can be carried out even for multi-dimensional integration problems.

To numerically check the multi-dimensional superefficiency of chaos-based Monte Carlo simulations, we consider a two-dimensional integrand as follows:

$$B(x,y) = xy - (2x^2 - 1)(4y^3 - 3y) = T_1(x)T_1(y) - T_2(x)T_3(y).$$

This integrand corresponds to $a_c = 0$, $a_0 = 1$, $a_1 = -1$, $p_1 = 2$, $p_2 = 3$ and L = 1 in Eq. (47). Thus, the superefficiency condition is satisfied. Therefore, if we use the chaotic dynamical systems $X_{j+1} = T_2(X_j)$ and $Y_{j+1} = T_3(Y_j)$ as random-number generators for x and y respectively, superefficient Monte Carlo computation is predicted to be carried out such that the numerically obtained expectation value of the square of the error V(N) is given by

$$V_{T_2,T_3}(N) \approx \sigma_{T_2,T_3}(N) = \frac{1}{2N^2},$$
 (51)

while the other chosen sets of chaotic dynamical systems yield

$$V_{T_{p1},T_{p2}}(N) \approx \sigma_{T_{p1},T_{p2}}(N) = \frac{1}{2N}$$
 (52)

for (p1, p2) = (2, 2), (3, 2), or, (3, 3). Figure 5 shows that the numerical data coincide well with our theory about the multi-dimensional superefficiency of chaosbased Monte Carlo simulations.

7 Superefficiency: A Case of Non-Gaussian Chaos

Let us consider an integration problem over the infinite support $\Omega_I = (-\infty, \infty)$ with density function $\rho_{NG}(x)$. In this case, Weierstrass's approximation theorem cannot be directly applied. However, when we consider a functional space

$$\mathcal{L}^{2}(\Omega_{I}, \rho_{NG}) = \{ f(x) | \int_{\Omega_{I}} |f(x)|^{2} \rho_{NG}(x) dx < \infty \}, \tag{53}$$

the chaos-based Monte Carlo integration of an integrand $f(x) \in \mathcal{L}^2(\Omega_I, \rho_{NG})$ can also be performed without any modification of the above algorithm. The Monte Carlo integration over the infinite support also has many applications such as the pricing of exotic options in financial markets. Furthermore, the problem of Monte Carlo integration over the infinite support is very important from the theoretical point of view of Monte Carlo computation, because we cannot directly use the usual uniform random-number generators but must consider some non-uniform random numbers over Ω_I . Usually, a procedure of Monte Carlo integration over the infinite support must include a transformation from the uniformly distributed random numbers to random numbers with non-uniform distributions such as the inverse method [14]. Here without resort to a transformation of random variables, we directly use certain ergodic dynamical systems with invariant probability measures over the infinite support $\Omega_I = (-\infty, \infty)$ as random-numbers generators over Ω_I . Such ergodic dynamical systems over the infinite support were systematically found from the multiplication formulas of $tan(\theta)$ and its related functions [15]. We can thus use these chaotic dynamical systems for this chaos-based Monte Carlo simulations over the infinite support Ω_I . Let us briefly explain ergodic mappings over Ω_I . As will be shown in Appendices C and D, by using the topological conjugacy relation with Chebyshev mappings T_l , we can derive an infinite number of ergodic transformations

$$F_l(y) = h^{-1} \circ T_l \circ h(y), \tag{54}$$

where h is a differential onto-mapping (diffeomorphism) such that $h: (-\infty, \infty) \to (-1, 1)$ is given by $h(y) = \frac{1}{\sqrt{1+|y|^{2\alpha}}} \operatorname{sgn}(y)$ for $\alpha > 0$. These ergodic mappings $\{F_l\}$ have the same invariant probability measure [15]

$$\rho_{NG}(y) = \frac{\alpha |y|^{\alpha - 1}}{\pi (1 + |y|^{2\alpha})}.$$
(55)

Furthermore, as will be shown in Appendix C, we can consider the corresponding orthonormal system of functions $\{P_l(y) \equiv T_l \circ h(y)\}$ satisfying the same orthogonal relation as the Chebyshev orthogonal polynomials as follows:

$$\int_{-\infty}^{\infty} P_i(y) P_j(y) \rho_{NG}(y) dy = \delta_{i,j} \frac{(1 + \delta_{i,0})}{2}.$$
 (56)

These orthogonal functions constitute a complete orthonormal system of functions in $\mathcal{L}^2(\Omega_I, \rho_{NG})$. Hence, as in constructing multidimensional integrals in

terms of Chebyshev polynomials where superefficiency condition is attained, chaos-based Monte Carlo simulations for a family of integrands

$$B(x_1, \dots, x_s) = a_c + \sum_{m=0}^{L} a_m P_{p_1^m}(x_1) \dots P_{p_s^m}(x_s),$$
 (57)

where an each dynamical variable $X_{i,j}$ associated with x_i is computed by $X_{i,j+1} = F_{p_i}(X_{i,j})$, are superefficient if the condition

$$\sum_{m=0}^{L} a_m = 0 (58)$$

is satisfied. Table 3 lists these transformations $\{F_l\}_{l=1,2,3}$ and their dual transformations $\{F_l^*\}_{l=1,2,3}$ over Ω_I and their related orthogonal functions $\{P_l(x)\}_{l=1,2,3}$ and $\{P_l^*(x)\}_{l=1,2,3}$ which were used for numerical simulations to attain the superefficiency over the infinite support. Figure 6(a) shows the graphs of ergodic transformations at $\alpha=1$. Figure 6(b) shows the graphs of the density functions $\rho_{NG}(x)$ in Eq. (76) over Ω_I at several different α . In Fig. 7, we show that superefficient Monte Carlo computations of one-dimensional integrands $B(x) = P_2(x) - P_1(x) = \frac{1-x^2}{1+x^2} - \frac{\operatorname{Sgn}(x)}{\sqrt{1+x^2}}$ and $B(x) = P_2^*(x) - P_1^*(x) = \frac{x^2-1}{x^2+1} - \frac{x}{\sqrt{1+x^2}}$ (see Table 3) are carried out by the corresponding second-order ergodic mappings $F_2(X)$ and $F_2^*(X)$ at $\alpha=1$. In Fig. 8, we show that the superefficiency of chaos-based Monte Carlo computation is carried out for a two-dimensional integral of an integrand

$$B(x,y) = P_2(x)P_3(y) - P_1(x)P_1(y) = \frac{(1-x^2)(1-3y^2)\operatorname{sgn}(y)}{(x^2+1)(1+y^2)^{\frac{3}{2}}} - \frac{\operatorname{sgn}(x)\operatorname{sgn}(y)}{\sqrt{1+x^2}\sqrt{1+y^2}}$$
(59)

(see also Table 3) over the infinite square $\Omega_2 = (-\infty, +\infty) \times (-\infty, \infty)$ when we use two different chaotic dynamical systems $X_{n+1} = F_2(X_n)$ and $Y_{n+1} = F_3(Y_n)$ at $\alpha = 1$ for the corresponding variables x and y of the two-dimensional integrand B(x, y). Hence, it is shown that chaos-based Monte Carlo computations can be performed to the integration problems over the infinite support by utilizing ergodic transformations over Ω_I and superefficient Monte Carlo computation can also be attained if the superefficiency condition is satisfied as before.

8 Physical Meaning of Superefficiency

Since the ergodic dynamical systems in this type of Monte Carlo computations generate Markov processes in [16], we can naturally construct stochastic processes obeying Brownian motion from the dynamical systems. We consider a random variable $\delta B_i \equiv B_i - \langle B \rangle = B(X_i) - \langle B(X_i) \rangle$ generated by a chaotic dynamical system $X_{n+1} = F(X_n)$ as a velocity of a Brownian particle at t = i. Here, the particle position of this discrete-time Brownian motion at t = N is given by

$$r(N) \equiv \sum_{i=0}^{N-1} \delta B_i = \sum_{i=0}^{N-1} \{ B_i - \langle B \rangle \}. \tag{60}$$

The diffusion coefficient $D_{discrete}$ is thus obtained by the formula

$$D_{\text{discrete}} \equiv \lim_{N \to \infty} \frac{\langle \langle r^2(N) \rangle \rangle}{2N} = \lim_{N \to \infty} \{N\sigma(N)\} = \frac{\langle B^2 \rangle - \langle B \rangle^2}{2} + \sum_{j=1}^{\infty} \{\langle B_0 B_j \rangle - \langle B \rangle^2\}.$$
(61)

In the second equality we used Eq. (8). Here, formula (61) can thus be seen as a discrete-time version of the formula

$$D_{\text{continuous}} \equiv \lim_{t \to \infty} \frac{\langle \langle r(t)^2 \rangle \rangle}{2t} = \int_0^\infty \langle u(0)u(t) \rangle dt, \tag{62}$$

for continuous-time Brownian motion $\{r(t)\}\$ with the particle velocity u(t) satisfying the Langevin equation

$$\dot{u}(t) = -\gamma u(t) + R(t) \tag{63}$$

where R(t) is assumed to be a Gaussian process such that

$$\langle \langle R(t) \rangle \rangle = 0, \langle \langle R(t)R(t') \rangle \rangle = 2\epsilon \delta(t - t')$$
 (64)

and $r(t) = \int_0^t u(t')dt'$. Hence, superefficiency condition (16) is simply rewritten as

$$D_{\text{discrete}} = \frac{\langle B^2 \rangle - \langle B \rangle^2}{2} + \sum_{j=1}^{\infty} \{ \langle B_0 B_j \rangle - \langle B \rangle^2 \} = 0.$$
 (65)

Note that $D_{\rm discrete}=0$ does not necessarily mean the corresponding discrete-time Brownian motion is dead, such as Brownian motion at zero temperature. As is clearly seen in Fig. 9, the discrete-time Brownian motion which corresponds to the superefficiency $D_{\rm discrete}=0$ is still actively fluctuating around zero without diffusing while the discrete-time Brownian motion corresponding to the normal Monte Carlo simulations, $D_{\rm discrete}>0$, has a normal diffusion behavior such as $\langle r^2(N)\rangle=O(N)$. We call such non-diffusing Brownian motion ultracoherent Brownian motion. This ultracoherent Brownian motion ($D_{\rm discrete}=0$) is quite unlike the zero diffusion ($D_{\rm continuous}=0$) case of continuous-time Brownian motion. Hence, the physical occurrence of the ultracoherent Brownian motion corresponding to the superefficient chaos Monte Carlo simulation is owing to the discrete nature of time in chaotic dynamical systems. Whether such ultracoherent Brownian motion is observed in real physical systems would be an interesting problem beyond the scope of the present paper.

9 Summary of the main results and conclusions

In this paper we show that Monte Carlo computation of a general multi-dimensional integrals are performed by various ergodic dynamical systems utilized as non-uniform random-number generators. Such chaos-based Monte Carlo computations exhibit a dynamical effect of random-number generations that cannot be

explained by the statistical arguments such as the importance sampling. By evaluating the expectation value $\sigma(N)$ of the square of the error in terms of two-point correlation functions, the dynamical dependency of chaotic randomnumber generations is shown to cause a non-negligible effect in Monte Carlo simulations. While an effect of chaotic random-number generations is generally seen as a variance reduction effect caused by negative covariance, we have shown that a superefficient Monte Carlo computation can be carried out such that the expectation value of the square of the error decreases to 0 in the order of $\frac{1}{N^2}$ with N successive observations for $N \to \infty$. Therefore, a proper choice of chaotic random-number generators to cause superefficiency greatly accelerates the speed of Monte Carlo computations. We have given the necessary and sufficient condition for achieving superefficient Monte Carlo computation. Interestingly, this superefficiency condition has a physical meaning such that the diffusion coefficient of the corresponding discrete-time Brownian motion constructed from chaotic random-number generators vanished ($D_{discrete} = 0$), where the Brownian particles move actively in a localized region around the expectation value of the Monte Carlo simulation. We numerically verified the superefficiency of chaos Monte Carlo computations which sharply depends on the integrand and our choice of chaotic dynamical systems as random-number generators under various settings of numerical integration problems. Thus we can see that observed dynamical dependency resulting in variance reduction in Section 3 is a partial realization of an extreme case of dynamical dependency, i.e., superefficiency.

Monte Carlo methods are widely used in various computational problems (such as calculating financial derivative securities, communication traffic analysis, optimization problems, and biological computations.) Therefore, such remarkably superior results from using chaotic correlation here give us to hope that they can effectively be applied to such hard computational problems. Furthermore, it is of special interest for us to investigate an possibility that some physical (or biological) computations with unknown mechanism such as fast protein-folding computation, would utilize the present kinds of superefficient Monte Carlo computation by the strong chaotic correlation of random-number generations.

In conclusion, the present paper shows that proper chaotic (ergodic) random-number generators have a distinguishable effect from the conventional pseudo random-number generators such that chaotic random-number generators can greatly accelerate the speed of convergence of the mean square error in Monte Carlo computation $(O(\frac{1}{N}) \to O(\frac{1}{N^2}))$ by utilizing negative correlation. Such superefficient Monte Carlo computation is robust under a change of the initial conditions, which is very promising for the application of chaotic random-number generators to many other computational problems, in which the expectation value of the square of the error is usually considered to slowly converge to 0 in the order of $O(\frac{1}{N})$.

Acknowledgements.

This work was initiated at the RIKEN Brain Science Institute. The author is grateful to S. Amari, Director of the Brain-Style Information Systems Research Group of the RIKEN Brain Science Institute for his generous support. The author would like to thank S. Amari, T. Khoda, T. Matsumoto, S. Tezuka, A. Yamaguchi, K. Goto, and T. Deguchi for their valuable discussions. The author wishes to express his gratitude to thank K. Kitayama, T. Itabe, and Y. Furuhama for their continuous encouragement. This work is, in part, supported by the CRL Scientific Research Fund from the Ministry of Posts and Telecommunications.

A Derivation of Eq. (8)

In this appendix, we derive formula (8).

$$\sigma(N) = \langle \langle [\overline{B}(N) - \overline{B}]^2 \rangle \rangle
= \langle \langle \overline{B}^2(N) \rangle \rangle - 2 \langle \langle \overline{B}(N) \overline{B} \rangle \rangle + \langle \langle \overline{B} \rangle \rangle^2
= \frac{1}{N^2} \sum_{j=0}^{N-1} \langle B_j^2 \rangle + \frac{2}{N^2} \sum_{j=1}^{N-1} (N-j) \langle B_0 B_j \rangle - 2 \langle \overline{B}^2 \rangle + \langle B \rangle^2
= \frac{1}{N} \langle B^2 \rangle + \sum_{j=1}^{N} \frac{2(N-j)}{N^2} \langle B_j B_0 \rangle - \langle B \rangle^2
= \frac{1}{N} \{ \langle B^2 \rangle - \langle B \rangle^2 \} + \frac{2}{N^2} \sum_{j=1}^{N} (N-j) \{ \langle B_0 B_j \rangle - \langle B \rangle^2 \}.$$

In the third equality, we used the invariance property:

$$\langle B[F(X)]\rangle = \langle B\rangle \tag{66}$$

and the following identities

$$\langle\langle \overline{B}(N)\rangle\rangle = \frac{1}{N} \sum_{j=0}^{N-1} \langle\langle B_j\rangle\rangle = \langle B\rangle = \overline{B}.$$
 (67)

In the last equality, we use the identity

$$\frac{2}{N^2} \sum_{j=1}^{N} (N-j) \langle B \rangle^2 = \langle B \rangle^2 - \frac{1}{N} \langle B \rangle^2.$$
 (68)

B Derivation of Eq. (49)

In this appendix, we derive formula (49).

Since the following equalities

$$2\sum_{l=1}^{N} (1 - \frac{l}{N}) \{ \langle B_0 B_l \rangle - \langle B \rangle^2 \} = \frac{1}{2^{s-1}} \sum_{l=1}^{L} (1 - \frac{l}{N}) \sum_{m=l}^{L} a_m a_{m-l}$$

$$= \frac{1}{2^s} \{ (\sum_{m=0}^{L} a_m)^2 - (\sum_{m=0}^{L} a_m^2) \} - \frac{1}{N2^{s-1}} \sum_{l=1}^{L} \sum_{m=l}^{L} a_m a_{m-l} l,$$

and

$$\langle B^2 \rangle - \langle B \rangle^2 = \frac{1}{2^s} \sum_{m=0}^L a_m^2,$$

hold, we have for $N \geq L$

$$\sigma(N) = \frac{1}{N} \{\langle B^2 \rangle - \langle B \rangle^2\} + \frac{2}{N} \sum_{l=1}^{N} (1 - \frac{l}{N}) \{\langle B_0 B_l \rangle - \langle B \rangle^2\}
= \frac{1}{N} \frac{\sum_{m=0}^{L} a_m^2}{2^s} + \frac{1}{N} \frac{\{(\sum_{m=0}^{L} a_m)^2 - \sum_{m=0}^{L} a_m^2\}}{2^s} - \frac{1}{2^{s-1}N^2} \sum_{l=1}^{L} \sum_{m=l}^{L} a_m a_{m-l} l
= \frac{1}{N} \frac{(\sum_{m=0}^{L} a_m)^2}{2^s} - \frac{1}{2^{s-1}N^2} \sum_{l=1}^{L} \sum_{m=l}^{L} a_m a_{m-l} l.$$

C Orthonormal System of Functions Related to the Topological Conjugacy Relation with Chebyshev Maps

In this appendix, we derive various orthonormal functions from ergodic mappings by using the topological conjugacy relations with Chebyshev polynomials. Let us consider the topological conjugacy relation with the Chebyshev maps $f \in \{T_m\}_{m=0,\cdots}$

$$\tilde{f}(y) = h^{-1} \circ f \circ h(y), \tag{69}$$

where \tilde{f} and f are onto-mappings such that $\tilde{f}:\Omega_I\to\Omega_I$ and $f:\Omega\to\Omega$, and h is a differentiable one-to-one mapping (diffeomorphism) as $h:\Omega_I\to\Omega$. Since h is a diffeomorphism, h preserves the ergodicity, and the mixing property of f; \tilde{f} also has a mixing (thus, ergodic) property if f has the mixing (thus, ergodic) property. Recall that the p-th Chebyshev maps at $p\geq 2$ have the invariant measures $\rho(x)dx=\frac{dx}{\sqrt{1-x^2}}$ and they satisfy the orthogonal relation with respect to this measure $\rho(x)dx$. Suppose that the mapping \tilde{f} has the invariant probability measure $\rho_{NG}(y)dy$. Then, the probability preservation relation

$$\rho(x)|dx| = \rho_{NG}(y)|dy| \tag{70}$$

holds. We thus obtain the density function $\rho_{NG}(y)$ for \tilde{f} as follows:

$$\rho_{NG}(y) = \rho[h(y)] \left| \frac{dh(y)}{dy} \right|. \tag{71}$$

Here we consider a system of mappings $\{F_l\}_{l=0,\dots,\infty}$ where F_l is defined by the topological conjugacy with the l-th order Chebyshev map

$$F_l(y) = h^{-1} \circ T_l \circ h(y). \tag{72}$$

Since the Chebyshev maps $\{T_l\}$ at $l \geq 2$ have the mixing property, all of the corresponding maps $\{F_l\}$ at ≥ 2 also have the mixing property. We therefore have the following theorem.

Theorem 2 A systems of functions $\{P_l(y)\}_{l=0,\dots,\infty}$ defined as

$$P_l(y) \equiv T_l[h(y)] = h^{-1}[F_l(y)]$$

constitutes an orthonormal system of functions such that

$$\int_{\Omega_I} P_i(y) P_j(y) \rho_{NG}(y) dy = \delta_{i,j} \frac{(1 + \delta_{i,0})}{2}, \tag{73}$$

where $\rho_{NG}(y)$ is a density function defined in Eq. (71).

The proof of the theorem is given by the following identity

$$\int_{\Omega_{I}} P_{i}(y)P_{j}(y)\rho_{NG}(y)dy = \int_{\Omega} h \circ F_{i} \circ h^{-1}(x) \cdot h \circ F_{j} \circ h^{-1}(x)\rho(x)dx$$

$$= \int_{\Omega} T_{i}(x) \cdot T_{j}(x)\rho(x)dx$$

$$= \delta_{i,j} \frac{(1+\delta_{i,0})}{2}.$$
(74)

In the last equality, we use the orthonormal property of the Chebyshev system in Eq. (21). The topological conjugacy relation with the Chebyshev maps thus gives the corresponding orthonormal system $\{P_l(y)\}$ with the density function $\rho_{NG}(y)$ as well as the corresponding ergodic mapping $F_l(y)$ with the invariant probability measure $\rho_{NG}(y)dy$.

D Non-Gaussian Chaos Mappings on the Real Line

In this appendix, we derive various ergodic transformations on the real line $(-\infty, \infty)$ via the topological conjugacy relations with the Chebyshev mappings $T_l(x)$. Let us consider a diffeomorphism $h: (-\infty, \infty) \to (-1, 1)$ given by

$$h(y) = \frac{1}{\sqrt{1 + |y|^{2\alpha}}} \operatorname{sgn}(y) \quad \text{for} \quad \alpha > 0.$$
 (75)

The topological conjugacy relation with the Chebyshev mappings T_l gives a set of infinite numbers of ergodic transformations $F_l(y) = h^{-1} \circ T_l \circ h(y)$ with the invariant measure $\rho_{NG}(y)dy$, where the density $\rho_{NG}(y)$ is given by the formula

$$\rho_{NG}(y) = \rho[h(y)] \left| \frac{h(y)}{dy} \right| = \frac{\alpha |y|^{\alpha - 1}}{\pi (1 + |y|^{2\alpha})}.$$
 (76)

Note that when $\alpha = 1$, the density function (76) corresponds to the Cauchy density function $\rho_{NG}(y) = \frac{1}{\pi(1+y^2)}$ with infinite variance. In general, density function (76) for $<\alpha < 2$ does not have a finite variance. As a result, the central limit theorem is not applicable here and then a superposition of random variables obeying this density does not converge in distribution to the Gaussian distribution but converge to the non-Gaussian Lévy's stable distribution[17]. Thus, we call these dynamical systems non-Gaussian chaos. Here, we consider a function f(x) as an integrand in the functional space $\mathcal{L}^2(\Omega_I, \rho_{NG})$ such as

$$\mathcal{L}^{2}(\Omega_{I}, \rho_{NG}) = \{ f(x) | \int_{\Omega_{I}} |f(x)|^{2} \rho_{NG}(x) dx < \infty \}, \tag{77}$$

which are spanned by the orthonormal system of functions $\{P_l(y)\}$. The functional space $\mathcal{L}^2(\Omega_I, \rho_{NG})$ for $0 < \alpha < 2$ is clearly different from the functional space $\mathcal{L}^2(\Omega_I, e^{-x^2})$ which can be spanned by the complete orthonormal system of the Hermite polynomials $H_l(x) = (-1)^l e^{x^2} \frac{d^l}{dx^l} e^{-x^2}$ with respect to the Gaussian measure $e^{-x^2} dx$. According to Ref. [15], we can consider an ergodic transformation $F_l(y)$ with the density (76) as the multiplication formula of $|\tan(\theta)|^{\frac{1}{\alpha}} \operatorname{sgn}[\cos(\theta)]$, that is,

$$F_l(|\tan(\theta)|^{\frac{1}{\alpha}}\operatorname{sgn}[\cos(\theta)]) = |\tan(l\theta)|^{\frac{1}{\alpha}}\operatorname{sgn}[\cos(l\theta)]. \tag{78}$$

In this way, we can easily obtain a series of ergodic transformations $\{F_l\}_{l=2,3,\cdots}$ with non-Gaussian density function over the infinite support $(-\infty, \infty)$ as follows:

$$F_2(y) = \left| \frac{2|y|^{\alpha}}{1 - |y|^{2\alpha}} \right|^{\frac{1}{\alpha}} \operatorname{sgn}(-|y|^{2\alpha} + 1), F_3(y) = \left| \frac{|y|^{\alpha}(|y|^{2\alpha} - 3)}{1 - 3|y|^{2\alpha}} \right|^{\frac{1}{\alpha}} \operatorname{sgn}[y(1 - 3|y|^{2\alpha})], \cdots.$$
(79)

In the same way as used in the preceding appendix, orthogonal functions $\{P_l(y)\}$ satisfying Eq. (73) with respect to the density $\rho_{NG}(y)$ over the infinite support $\Omega_I = (-\infty, \infty)$ are derived as follows:

$$P_0(y) = 1, P_1(y) = h(y), P_2(y) = \frac{-|y|^{2\alpha} + 1}{|y|^{2\alpha} + 1}, P_3(y) = \frac{1 - 3|y|^{2\alpha}}{(1 + |y|^{2\alpha})^{\frac{3}{2}}} \operatorname{sgn}(y), \cdots$$
(80)

On the contrary, if we choose a diffeomorphism $h^*: \Omega_I \to \Omega$ given by

$$h^*(y) = \frac{|y|^{\alpha}}{\sqrt{1 + |y|^{2\alpha}}} \cdot \operatorname{sgn}(y), \tag{81}$$

the corresponding ergodic transformations $F_l^*(y)$ are derived from the Chebyshev mappings $T_l(y)$ via the topological conjugacy relation

$$h^* \circ F_l^*(y) = T_l \circ h^*(y).$$
 (82)

In this case, F_l^* is equivalent to a multiplication formula of $|\cot(\theta)|^{\frac{1}{\alpha}} \operatorname{sgn}[\cos(\theta)]$ as

$$F_l^*(|\cot(\theta)|^{\frac{1}{\alpha}}\operatorname{sgn}[\cos(\theta)]) = |\cot(l\theta)|^{\frac{1}{\alpha}}\operatorname{sgn}[\cos(l\theta)]. \tag{83}$$

We thus obtain a series of ergodic transformations $\{F_l^*(y)\}$ such that

$$F_2^*(y) = \left| \frac{1}{2} (|y|^{\alpha} - \frac{1}{|y|^{\alpha}}) \right|^{\frac{1}{\alpha}} \operatorname{sgn}(|y| - \frac{1}{|y|}), F_3^*(y) = \left| \frac{|y|^{\alpha} (3 - |y|^{2\alpha})}{1 - 3|y|^{2\alpha}} \right|^{\frac{1}{\alpha}} \operatorname{sgn}[y(|y|^{2\alpha} - 3)], \cdots.$$
(84)

Correspondingly, orthogonal functions $\{P_l^*(y)\}$ related to the transformations $\{F_l^*(y)\}_{l=0,\dots}$ are derived as follows:

$$P_0^*(y) = 1, P_1^*(y) = h^*(y), P_2^*(y) = \frac{|y|^{2\alpha} - 1}{|y|^{2\alpha} + 1}, P_3^*(y) = \frac{|y|^{\alpha}(|y|^{2\alpha} - 3)}{(1 + |y|^{2\alpha})^{\frac{3}{2}}} \operatorname{sgn}(y), \cdots.$$
(85)

In the construction of the above ergodic mappings, there exists a duality such that

$$F_l(y)F_l^*(z) = 1$$
, for $yz = 1$. (86)

Table 3 summarizes the analytical results here for the ergodic transformations and the related orthogonal functions, which are necessary for producing the numerical results of the superefficient chaos Monte Carlo computations over the infinite support Ω_I in Section 7. The graphs of ergodic transformations over Ω_I are depicted in Fig. 6(a).

References

- [1] D. E. Knuth, The Art of Computer Programming: Vol. 2, Seminumerical Algorithms (Addison-Wesley, Reading, MA, 1969).
- [2] S. C. Phatak and S. Suresh Rao, Phys. Rev. E 51 (1995) 3670.
- [3] K. Binder and D. W. Heermann, Monte Carlo Simulation in Statistical Physics (Springer, 1988).
- [4] G. S. Fishman, Monte Carlo Concepts, Algorithms, and Applications (Springer, 1996)
- [5] N. Metropolis, in *From Cardinals to Chaos*, edited by N. G. Cooper, p. 125-130. (Cambridge Univ. Press, 1989).
- [6] S. M. Ulam and J. von Neumann, Bull. Am. Math. Soc. 53 (1947) 1120.

- [7] R. L. Adler and T. J. Rivlin, *Proc. Am. Math. Soc.* **15** (1964) 794.
- [8] K. Umeno, *Phys. Rev.* E **55** (1997) 5280 (eprint chao-dyn/961009).
- [9] K. Umeno, Exactly solvable chaos and addition theorems of elliptic functions, (eprint chao-dyn/9704007).
- [10] G.D. Birkhoff, Proc. Nat. Acad. Sci. USA 17 (1931) 656.
- [11] J. M. Hammersley and K.W. Morton, Proc. Camb. Phil. Soc. **52** (1956) 449.
- [12] H. Niederreiter, Random Number Generation and Quasi-Monte Carlo Methods (SIAM, Philadelphia, 1992).
- [13] R. Courant and D. Hilbert, Methoden der Mathematischen Physik, vol 1. (Springer 2d ed: Berlin, 1931).
- [14] L. Devroye, Non-Uniform Random Variate Generation, (Springer, 1986).
- [15] K. Umeno, Phys. Rev. E58 (1998) 2644 (eprint chao-dyn/9711023).
- [16] A. Lasota and M. C. Mackey, *Chaos, Fractals, and Noise* (Springer, 1994, second edition).
- [17] B. V. Gnedenko and A. N. Kolmogorov, Limit Distributions for Sums of Independent Random Variables (Addison-Wesley, Reading, MA, 1954).

Table 1: Ergodic Mappings with Lyapunov exponents λ on [0,1]

Rational Mappings on [0,1]	Densities $\rho(x)$	λ
$f^{(2)}(x) = 4x(1-x) \text{ (Ulam-von Neumann Map)[6]}$	$\frac{1}{\pi\sqrt{x(1-x)}}$	ln2
$f^{(3)}(x) = x(3-4x)^2 \text{ (Cubic Map)[7]}$	$\frac{1}{\pi\sqrt{x(1-x)}}$	ln3
$f^{(5)}(x) = x(5 - 20x + 16x^2)^2 (\text{Quintic Map})[7]$	$\frac{1}{\pi\sqrt{x(1-x)}}$	ln5
$f_{l,m}^{(2)}(x) = \frac{4x(1-x)(1-lx)(1-mx)}{1-2(l+m+lm)x^2+8lmx^3+(l^2+m^2-2lm-2l^2m-2lm^2+l^2m^2)x^4}[8]$	$\frac{1}{K\sqrt{x(1-x)(1-lx)(1-mx)}}$	ln2
$f_{l,m}^{(3)}(x) = \left[x\{-3 + 4x + 4(l+m)x - 6(l+m+lm)x^2 + 12lmx^3 + (l^2 + m^2 - 2lm - 2l^2m - 2lm^2 + l^2m^2)x^4\}^2\right]/$	$\frac{1}{K\sqrt{x(1-x)(1-lx)(1-mx)}}$	ln3
$ [1 - 12(l + m + lm)x^{2} + 8(l + m + l^{2} + m^{2} + l^{2}m + lm^{2})x^{3} $ $ + 120lmx^{3} + 6(5l^{2} + 5m^{2} - 26lm - 26l^{2}m - 26lm^{2} + 5l^{2}m^{2})x^{4} $ $ + 24(-2l^{2} - 2m^{2} - 2l^{3} - 2m^{3} + 4lm + 7l^{2}m + 7lm^{2})x^{5} $ $ + 24(4l^{3}m + 4lm^{3} + 7l^{2}m^{2} - 2l^{3}m^{2} - 2l^{2}m^{3})x^{5} $ $ + 4(4l^{2} + 4m^{2} + 4l^{4} + 4m^{4} + 17l^{3} + 17m^{3} - 8lm)x^{6} $	•	
$ +4(-17l^{2}m - 17lm^{2} - 17l^{3}m - 17lm^{3} - 8l^{4}m - 8lm^{4})x^{6} $ $+4(4l^{2}m^{4} + 4l^{4}m^{2} - 17l^{3}m^{2} - 17l^{2}m^{3} + 17l^{3}m^{3} - 54l^{2}m^{2})x^{6} $ $+24(-l^{3} - m^{3} - l^{4} - m^{4} + l^{2}m + lm^{2} - l^{3}m - lm^{3})x^{7} $ $+24(l^{4}m + lm^{4} + 4l^{2}m^{2} + 4l^{3}m^{2} + 4l^{2}m^{3})x^{7} $ $+24(l^{4} - 2 + l^{2} - l^{4} - l^{3} - l^{3} - l^{4} - l^{3} - l^{3} - l^{4} - l^{3} - l^{4} - l^{3} - l^{4} -$		
$ +24(l^{4}m^{2} + l^{2}m^{4} - l^{3}m^{3} - l^{4}m^{3} - l^{3}m^{4})x^{7} +3(3l^{4} + 3m^{4} + 4l^{3}m + 4lm^{3} + 4l^{4}m + 4lm^{4} - 14l^{2}m^{2})x^{8} +3(-4l^{3}m^{2} - 4l^{2}m^{3} - 4l^{3}m^{3} - 14l^{4}m^{2} - 14l^{2}m^{4})x^{8} +3(4l^{4}m^{3} + 4l^{3}m^{4} + 3l^{4}m^{4})x^{8} +8(-l^{4}m - lm^{4} + l^{3}m^{2} + l^{2}m^{3} + l^{4}m^{2} + l^{2}m^{4})x^{9} +8(-2l^{3}m^{3} + l^{4}m^{3} + l^{3}m^{4} - l^{4}m^{4})x^{9}] [8] $		

Table 2: Convergence speed of various types of Monte Carlo simulations with s-dimensional integration problems

Random-Number Generators	Variance of Error	
Standard Arithmetical Pseudo-Random Numbers (General)	$V(N) = O(\frac{1}{N})$	
Quasi-Random Numbers (General)	$V(N) = O\left[\frac{1}{N^2} \cdot (\ln N)^{2s}\right]$	
Superefficient Chaos Monte Carlo [under Condition (16)]	$V(N) = O(\frac{1}{N^2})$	
Chaos Monte Carlo (General)	$V(N) = O(\frac{1}{N})$	

Table 3: Orthogonal functions related to exactly solvable chaos

Index	$P_l(x)$	$F_l(x)$	Lyapunov Exponents
l=1	$\frac{1}{\sqrt{1+ x ^{2\alpha}}}\mathrm{sgn}(x)$	x	0
l = 1*(Dual)	$\frac{ x ^{\alpha}}{\sqrt{1+ x ^{2\alpha}}}\mathrm{sgn}(x)$	x	0
l=2	$\frac{- x ^{2\alpha}+1}{ x ^{2\alpha}+1}$	$\left \frac{2 x ^{\alpha}}{1- x ^{2\alpha}} \right ^{\frac{1}{\alpha}} \operatorname{sgn}(- x ^{2\alpha} + 1)$	ln2
l = 2*(Dual)	$\frac{ x ^{2\alpha}-1}{ x ^{2\alpha}+1}$	$ \frac{1}{2}(x ^{\alpha} - \frac{1}{ x ^{\alpha}}) ^{\frac{1}{\alpha}}\operatorname{sgn}(x - \frac{1}{ x }) $	ln2
l=3	$\frac{1-3 x ^{2\alpha}}{(1+ x ^{2\alpha})^{\frac{3}{2}}}\operatorname{sgn}(x)$	$\left \frac{ x ^{\alpha}(x ^{2\alpha} - 3)}{1 - 3 x ^{2\alpha}} \right ^{\frac{1}{\alpha}} \operatorname{sgn}[x(1 - 3 x ^{2\alpha})]$	ln3
l = 3*(Dual)	$\frac{ x ^{\alpha}(x ^{2\alpha}-3)}{(1+ x ^{2\alpha})^{\frac{3}{2}}}\operatorname{sgn}(x)$	$\left \frac{ x ^{\alpha}(3- x ^{2\alpha})}{1-3 x ^{2\alpha}}\right ^{\frac{1}{\alpha}}\operatorname{sgn}[x(x ^{2\alpha}-3)]$	ln3

Figure Captions

- Fig. 1.(a) The expectation values of the square of the errors for the chaos-based Monte Carlo computations of $\int_0^1 x^3 dx = \frac{1}{4}$ are plotted for various ergodic transformations listed in Table 1 on the unit interval [0,1]. A yellow line indicates a Monte Carlo computation utilizing pseudo-random numbers with a density $\rho(x) = \frac{1}{\sqrt{x(1-x)}}$ constructed from the uniform random-number generators (in Fortran 90 Library) by the inverse method. Thus, it can be seen that chaotic random-number generators reduce the error variance from the existence of dynamical correlation.
- (b) The expectation values of the square of the errors for the chaos Monte Carlo computations of $\int_0^1 x(1-x)dx = \frac{1}{6}$ are plotted for various ergodic transformations listed in Table 1 on the unit interval [0,1]. A yellow line indicates a Monte Carlo computation utilizing pseudo-random numbers with a density $\rho(x) = \frac{1}{\sqrt{x(1-x)}}$ constructed from the uniform random-number generators (in Fortran 90 Library) by the inverse method. Thus, it can be seen that chaotic random-number generators reduce the error variance from the existence of dynamical correlation.
- Fig. 2. The log-log plot of the expectation value of the square of the error for the chaos Monte Carlo computations of the one-dimensional integral with the integrand $B(x) = T_1(x) T_2(x)$ where the p-th order Chebyshev maps are utilized as non-uniform random-number generators over the interval [-1,1] for p = 2, 3, 4, 5. A superefficient Monte Carlo computation is carried out for the second order Chebyshev map $T_2(X)$.
- Fig. 3. The log-log plot of the expectation value of the square of the error for the chaos Monte Carlo computations of the one-dimensional integral with the integrand $B(x) = T_1(x) T_4(x)$ over [-1, 1] where the p-th order Chebyshev maps are utilized as non-uniform random-number generators for p = 2, 3, 4, 5. Superefficient Monte Carlo computations are carried out for the second order Chebyshev map $T_2(X)$ and the fourth order Chebyshev map $T_4(X)$.
- Fig. 4.(a) The expectation values of the square of the error for superefficient Monte Carlo computations of the one-dimensional integral with the integrand $B(x) = T_1(x) T_4(x) + 1$ over [-1, 1] are plotted. The p-th order Chebyshev maps are utilized as non-uniform random-number generators at p = 2, 3, 4, 5. The initial conditions M = 1000 are generated according to a Chebyshev map with the invariant probability measure $\rho(x) = \frac{1}{\sqrt{1-x^2}}$.
- (b) The expectation value of the square of the error for superefficient Monte

Carlo computations of the one-dimensional integral with the integrand $B(x) = T_1(x) - T_4(x) + 1$ over [-1, 1] are plotted. The *p*-th order Chebyshev maps are utilized as non-uniform random-number generators at p = 2, 3, 4, 5. The initial conditions M = 1000 are distributed according to the uniform pseudo-random numbers over the domain $\Omega = [-1, 1]$.

- Fig. 5. The log-log plot of the expectation value of the square of the error for the chaos Monte Carlo computations of the two-dimensional integral $B(x,y) = T_1(x)T_1(y) T_2(x)T_3(y)$ over the domain $\Omega_2 = [-1,1] \times [-1,1]$ in the case that the p-th order Chebyshev maps are utilized as non-uniform random-number generators at p = 2,3. A superefficient Monte Carlo computation is carried out for the second order Chebyshev map $T_2(X)$ for the x variable and the third order Chebyshev map $T_4(Y)$ for the y variable.
- Fig. 6(a) Non-Gaussian chaos mappings for $\alpha = 1$. All of the chaotic dynamical systems have the Cauchy distribution as the invariant probability measure.
- (b) Density functions of the invariant measures of non-Gaussian chaos mappings are plotted for $\alpha = \frac{1}{2}, 1, \frac{3}{2}, 2, 4$, and 10.
- Fig. 7 The log-log plot of the expectation value of the square of the error for the chaos Monte Carlo computations of the one-dimensional integrals $B(x) = P_2(x) P_1(x) = \frac{1-x^2}{1+x^2} \frac{\operatorname{sgn}(x)}{\sqrt{1+x^2}}$ and $B(x) = P_2^*(x) P_1^*(x) = \frac{x^2-1}{x^2+1} \frac{x}{\sqrt{1+x^2}}$ over the infinite support $(-\infty, \infty)$ where the second-order non-Gaussian chaos mappings $F_2(x)$ and $F_2^*(x)$ at $\alpha = 1$ in Table 3 are utilized as non-uniform random-number generators over $(-\infty, \infty)$. Superefficient Monte Carlo computations are carried out for the corresponding second-order non-Gaussian chaos maps $F_2(X)$ and $F_2^*(X)$ respectively.
- Fig. 8 The log-log plot of the expectation value of the square of the error for the chaos Monte Carlo computations of the two-dimensional integral with the integrand $B(x,y) = P_1(x)P_1(y) P_2(x)P_3(y)$ in Eq.(59) over the two-dimensional infinite support $(-\infty,\infty)\times(-\infty,\infty)$ where the second-order non-Gaussian chaos mapping F_2 and the third-order non-Gaussian chaos mapping F_3 at $\alpha=1$ are utilized as non-uniform random-number generators over $(-\infty,\infty)$. A superefficient Monte Carlo computation is carried out for the second order non-Gaussian chaos map $F_2(X)$ and the third order non-Gaussian chaos map $F_3(Y)$.
- Fig. 9(a) The Brownian motions generated by the Chebyshev maps which compute the integral of $B(x) = T_1(x) T_4(x)$ are plotted. The ordinate indicates an empirical mean defined by $S(N) \equiv \frac{1}{\sqrt{M}} \sum_{j=1}^{M} \sum_{i=0}^{N-1} [B_i(j) \langle B \rangle]$ for

M=1000. The initial data $\{X_0\}_{j=1,\cdots,M}$ are generated by a Chebyshev map with an invariant measure $\rho(x)dx=\frac{dx}{\sqrt{1-x^2}}$. Superefficient chaos-based Monte Carlo computations (the second order Chebyshev map $T_2(X)$ and the fourth order Chebyshev map $T_4(X)$), corresponds to the Brownian motions showing a very coherent behavior around the integral $\langle B(x) \rangle = 0$.

(b) The magnification of Fig. 9(a) around $0 \le N \le 1000$.

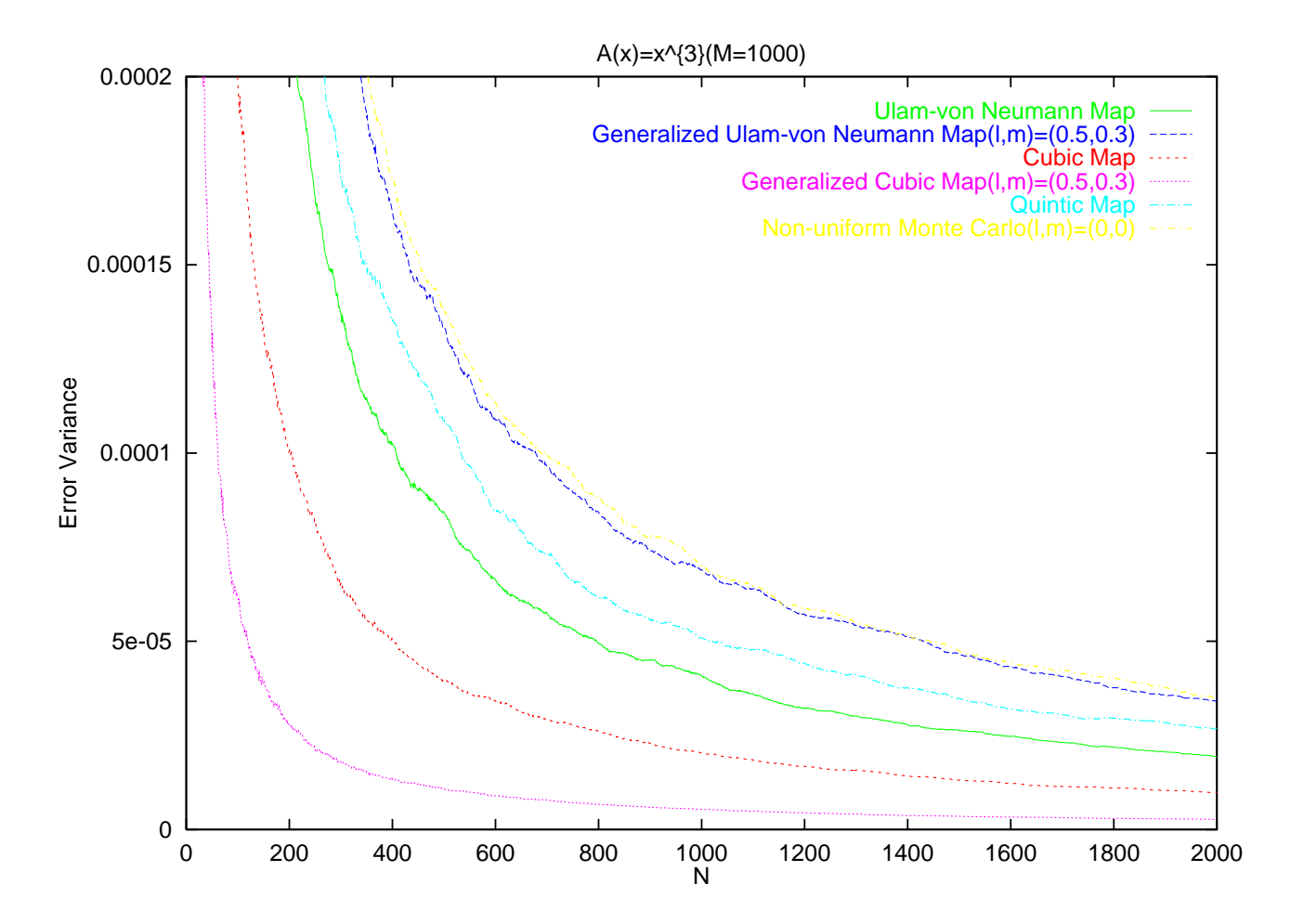


Fig. 1(a) Ken Umeno

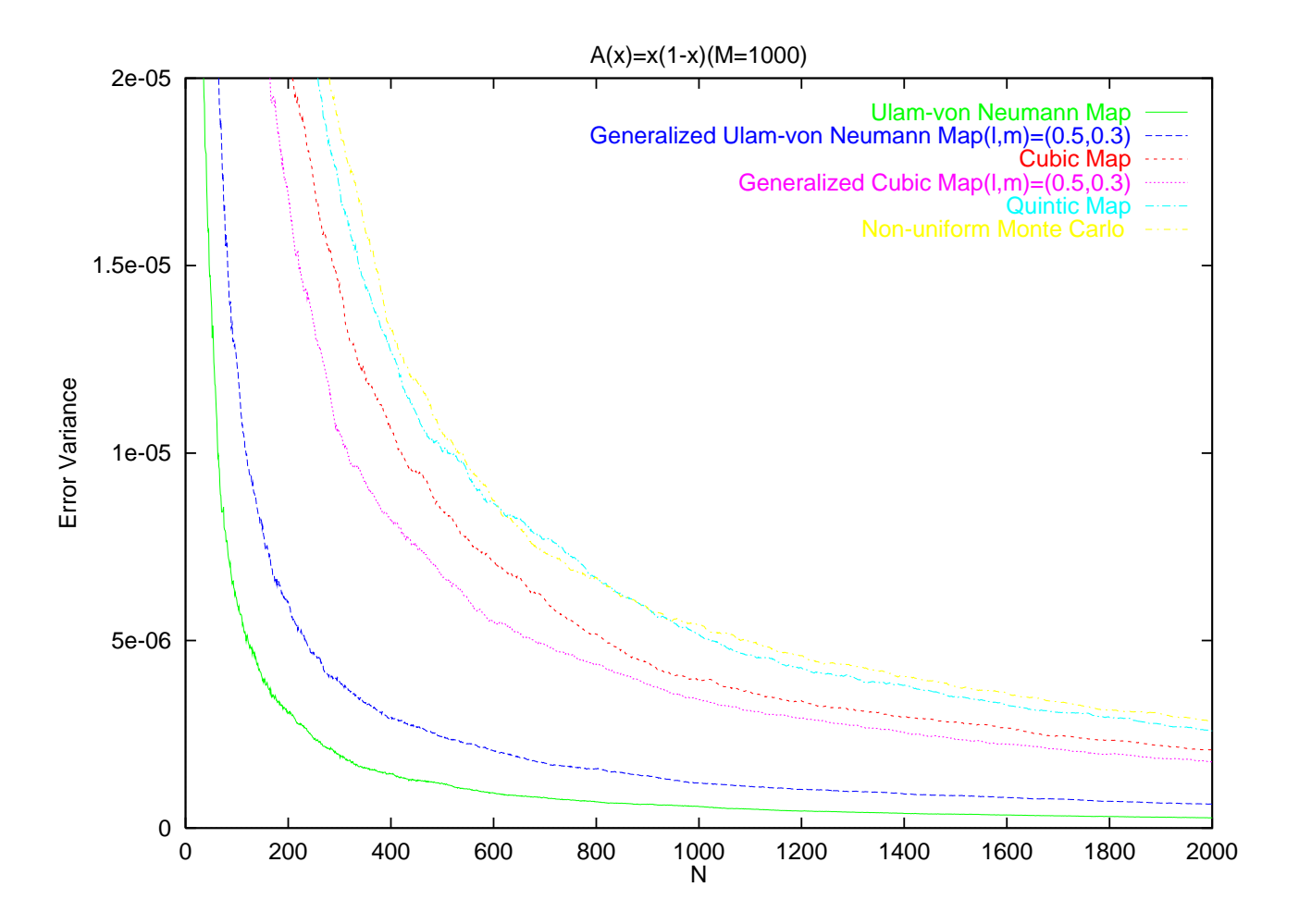


Fig. 1(b) Ken Umeno

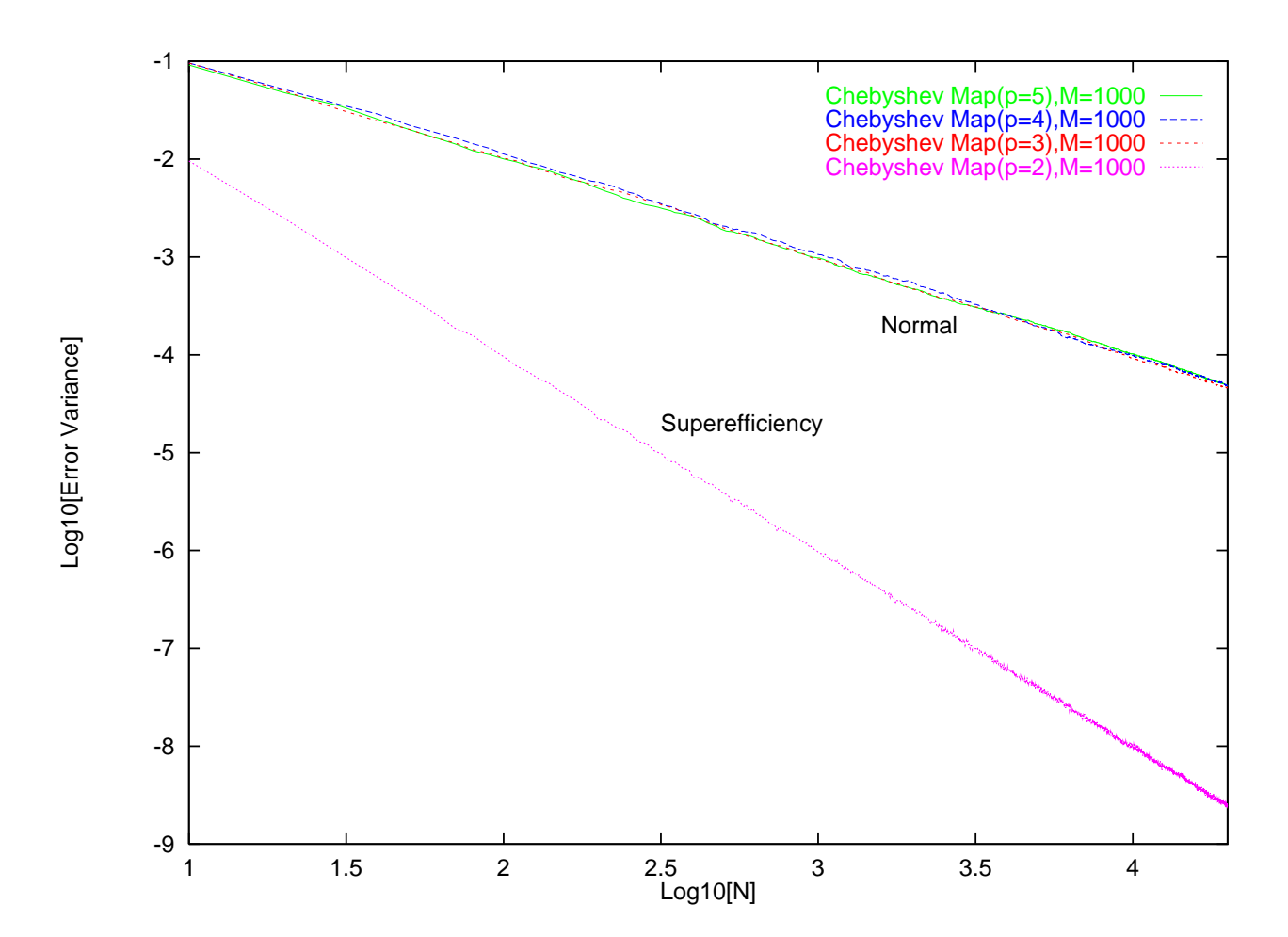


Fig. 2 Ken Umeno

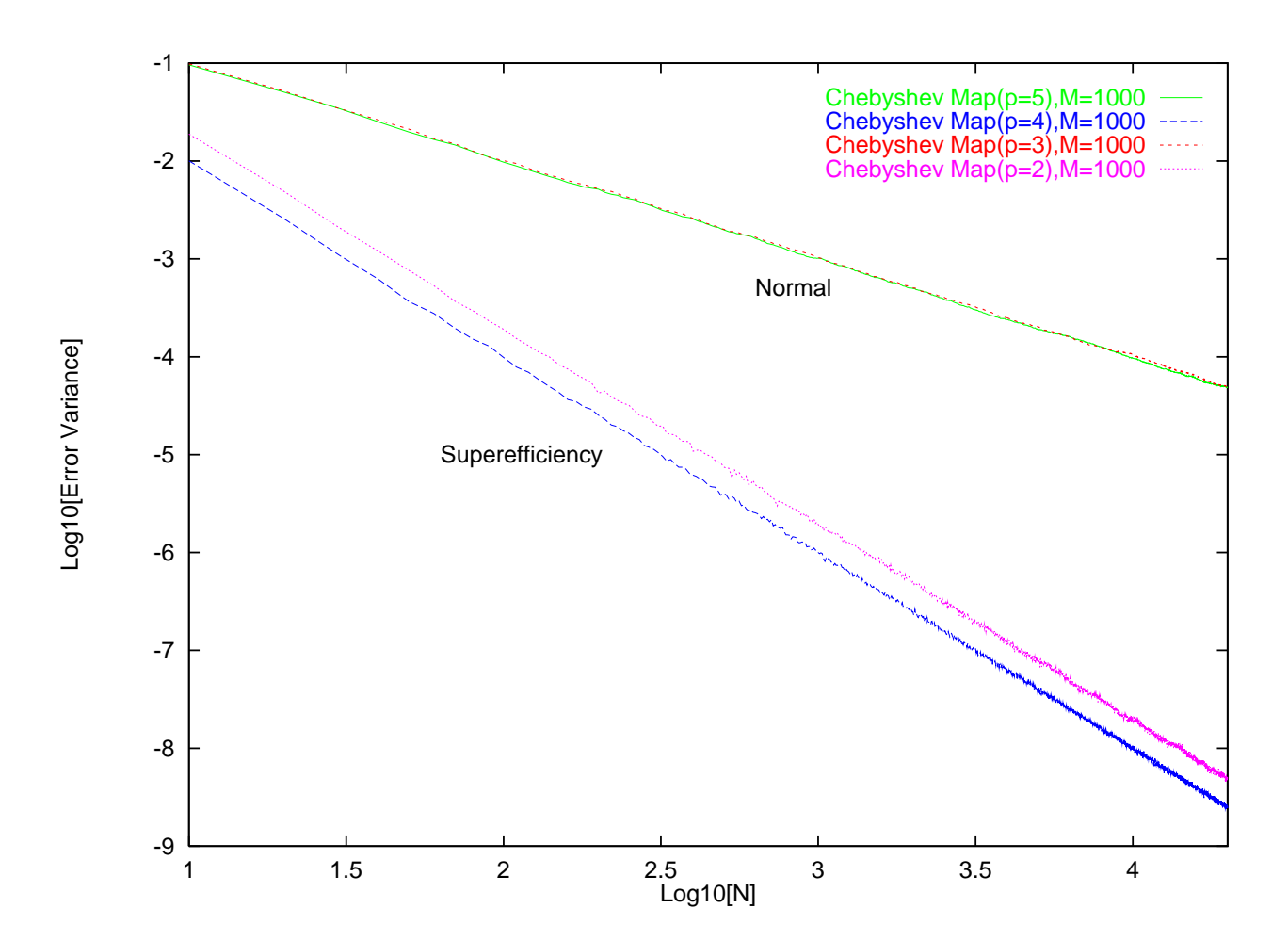


Fig. 3 Ken Umeno

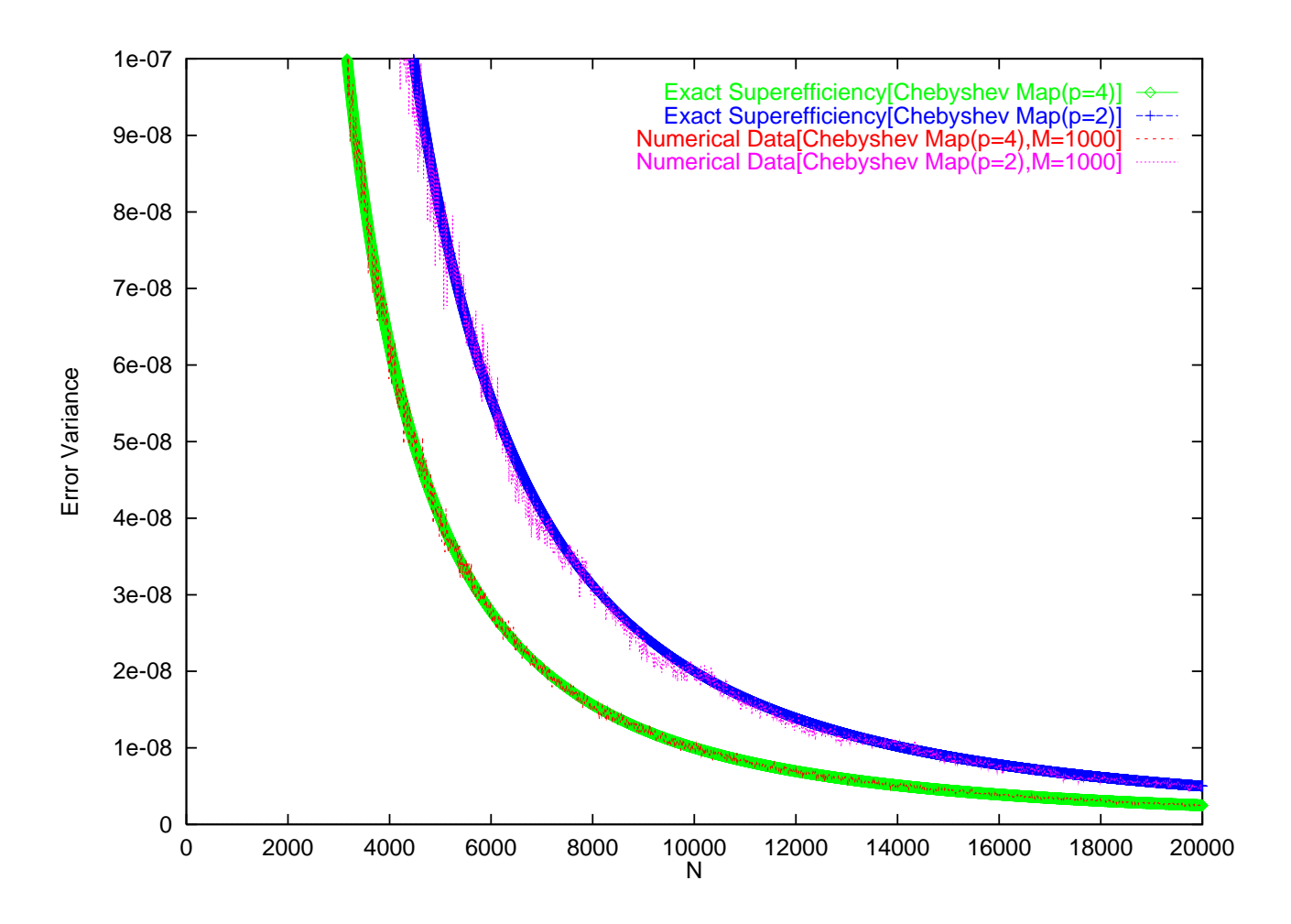


Fig. 4(a) Ken Umeno

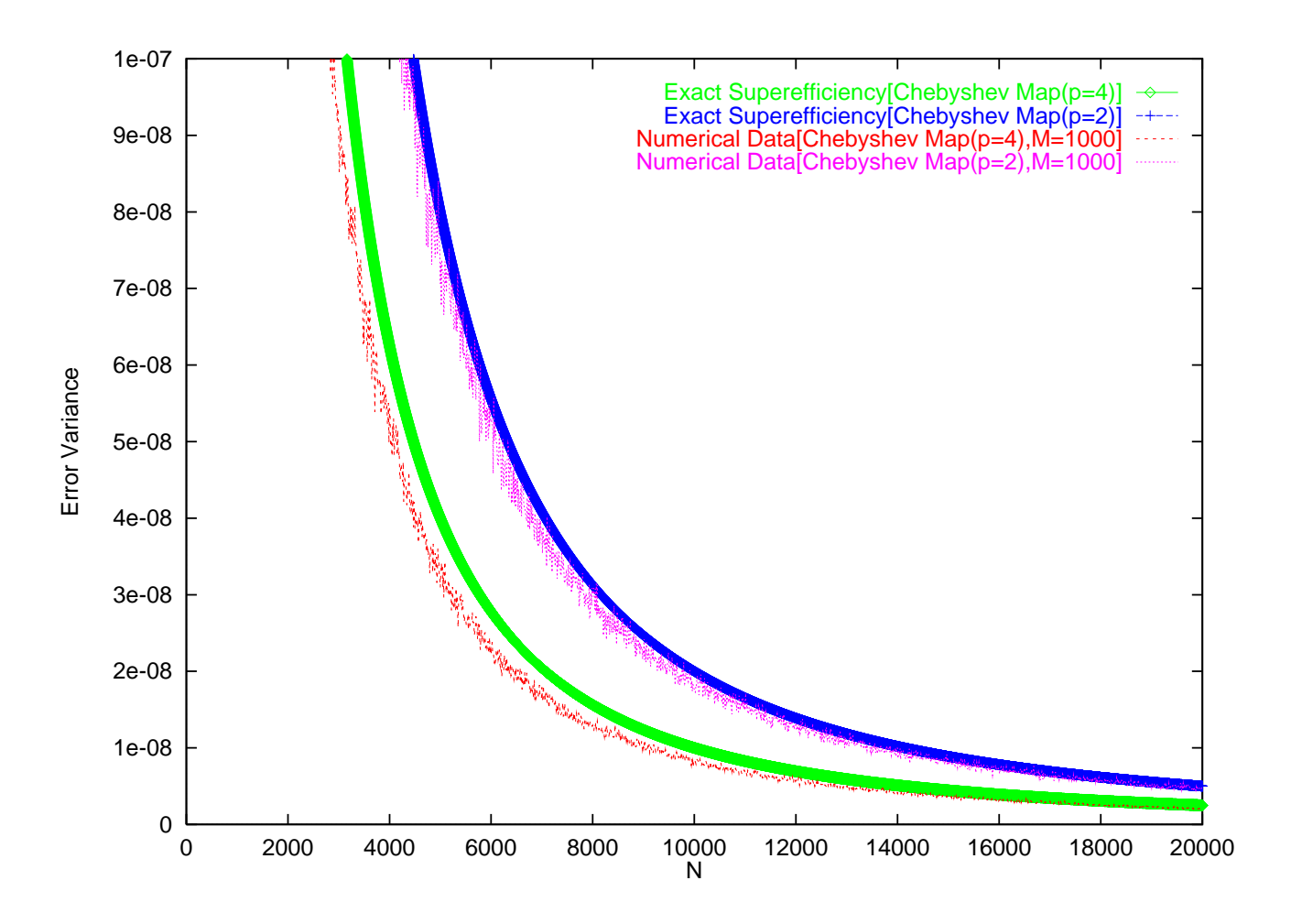


Fig. 4(b) Ken Umeno

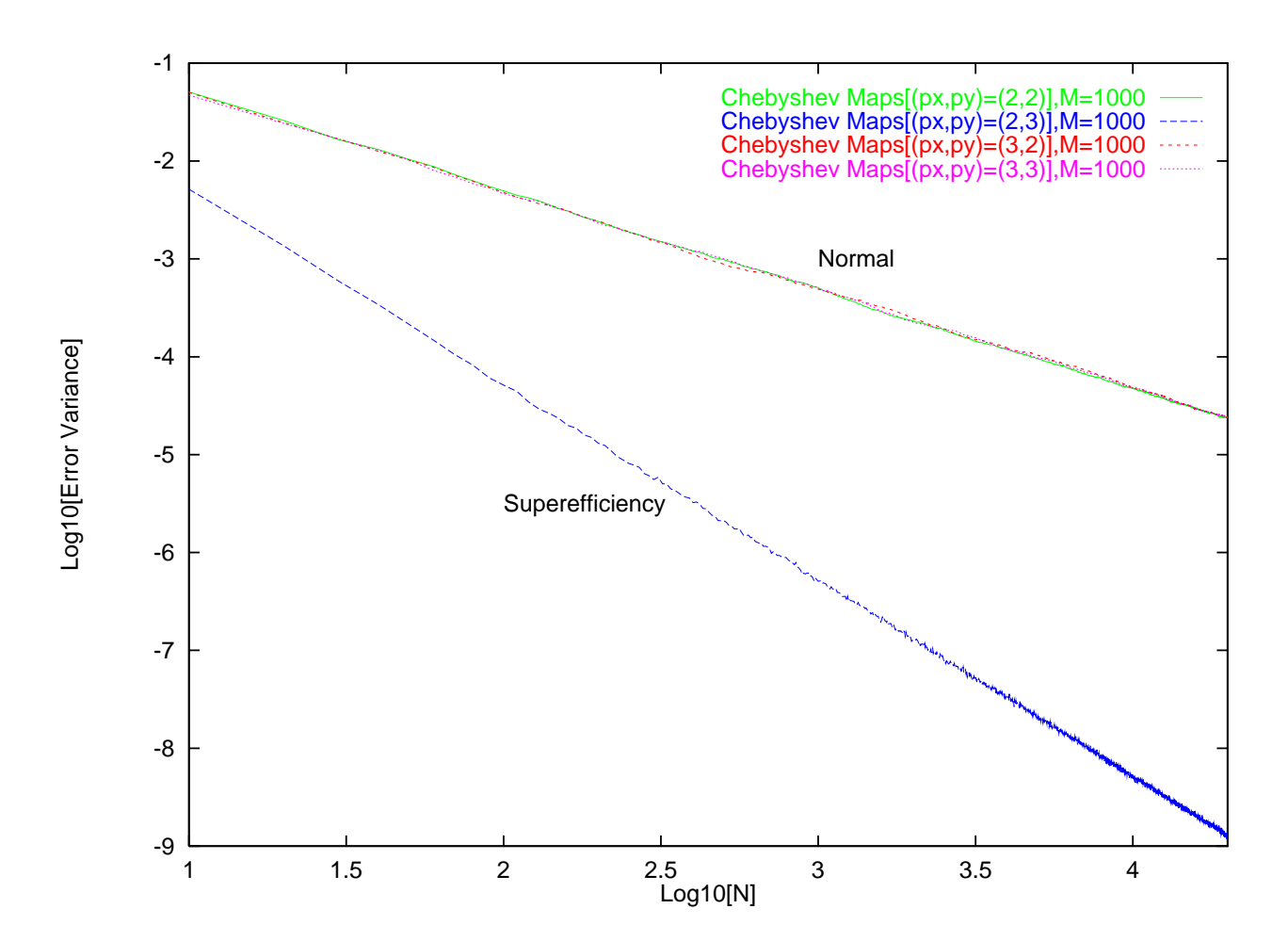


Fig. 5 Ken Umeno

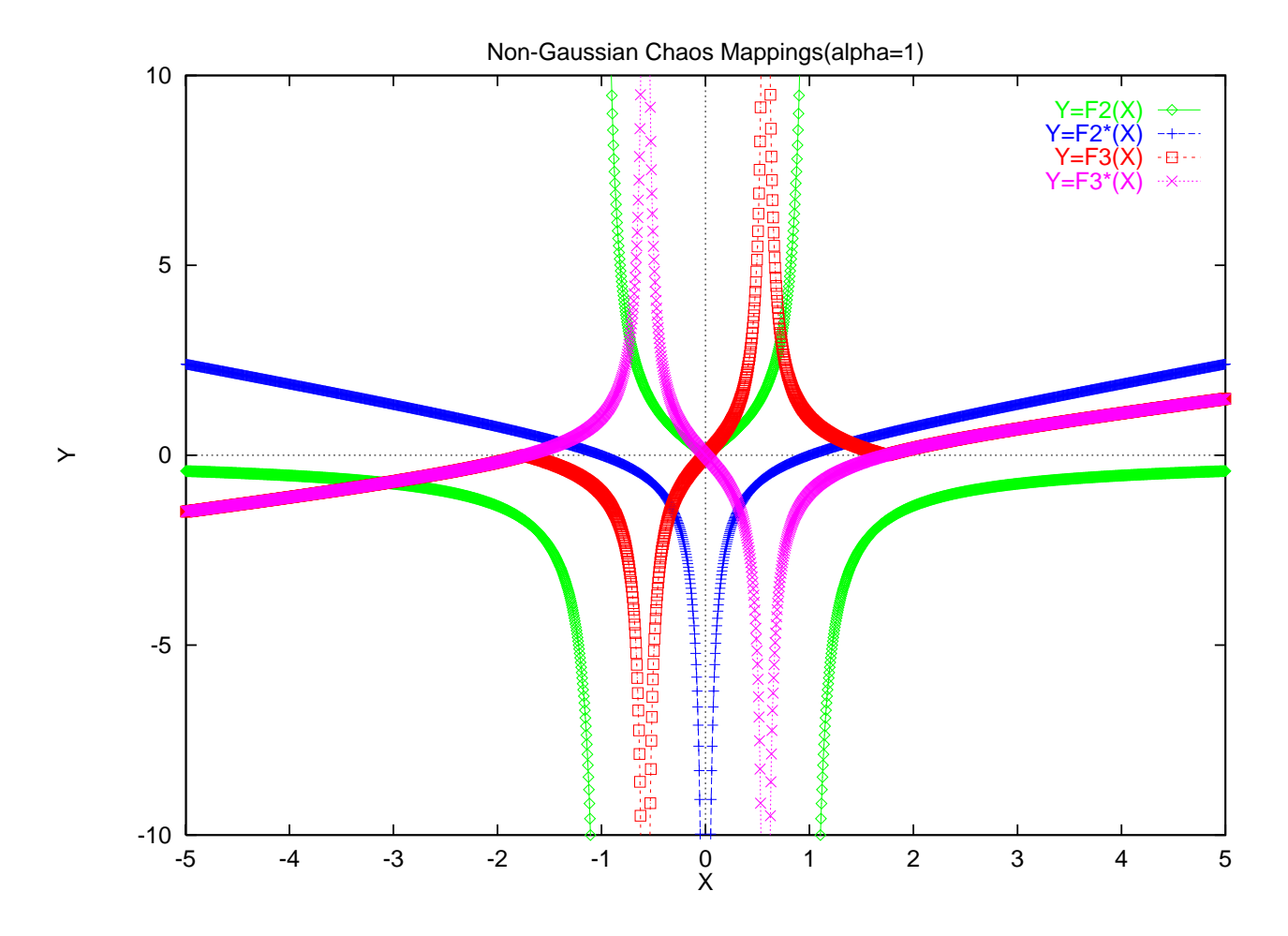


Fig. 6(a) Ken Umeno

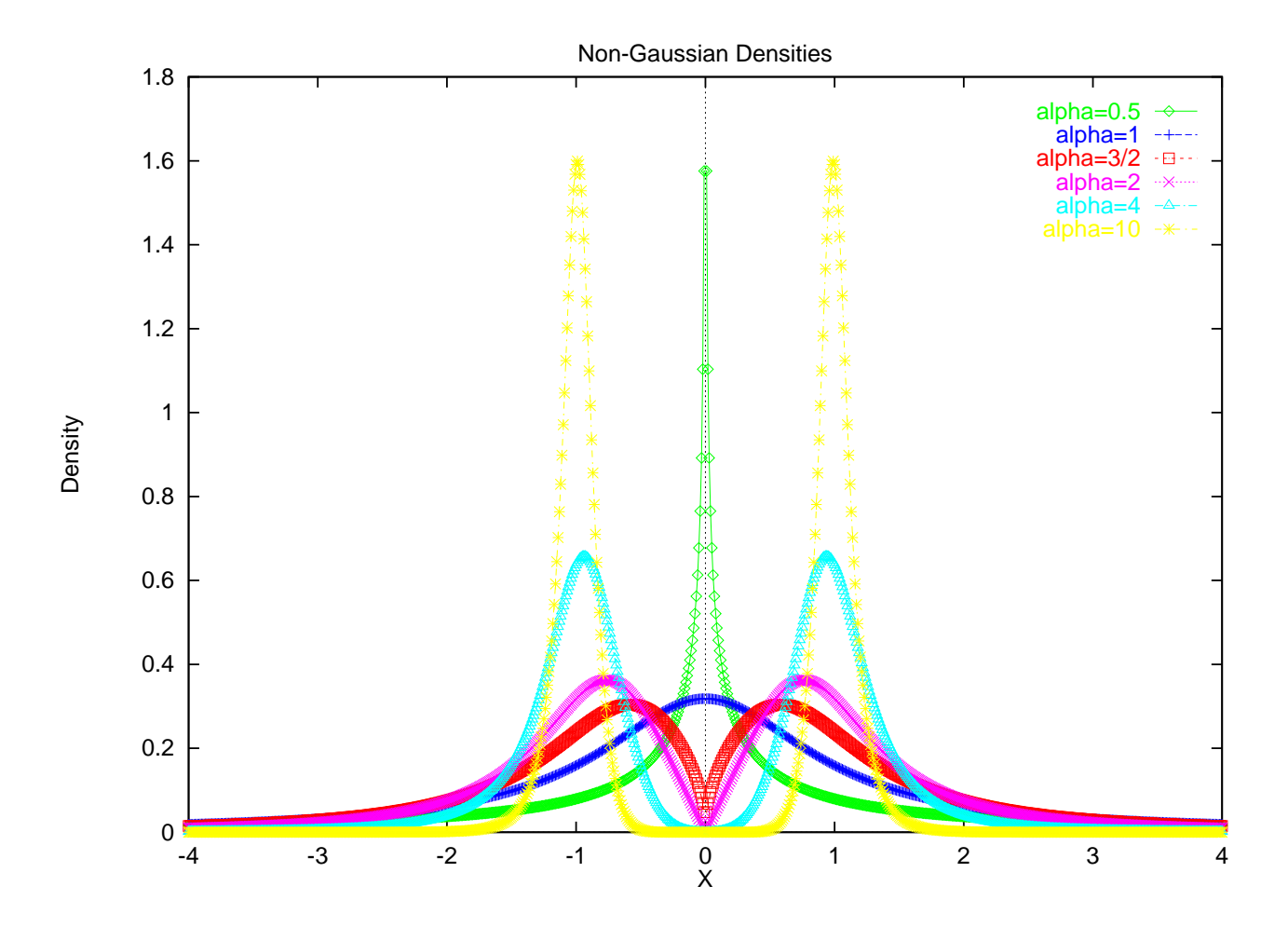


Fig. 6(b) Ken Umeno

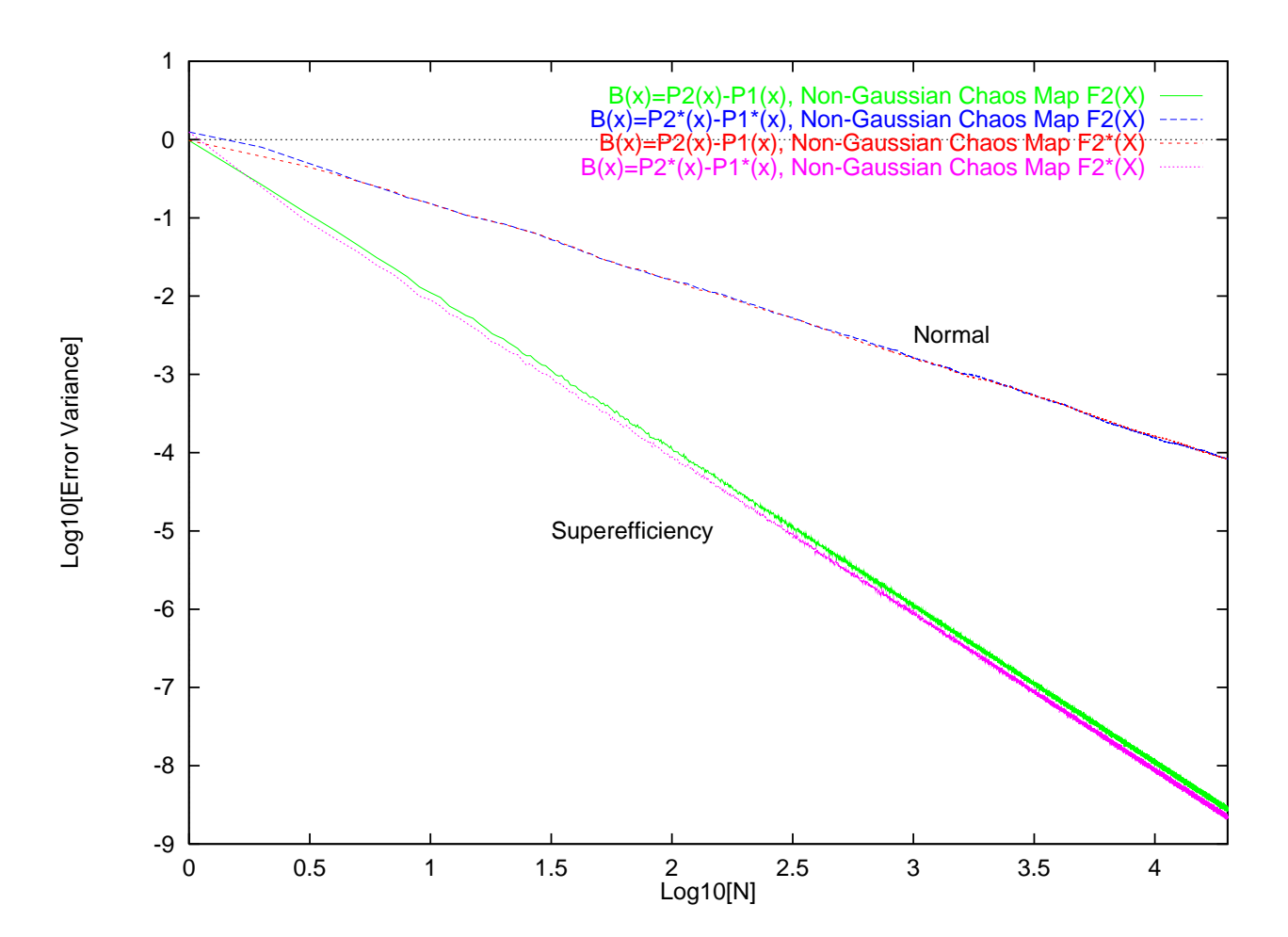


Fig. 7 Ken Umeno

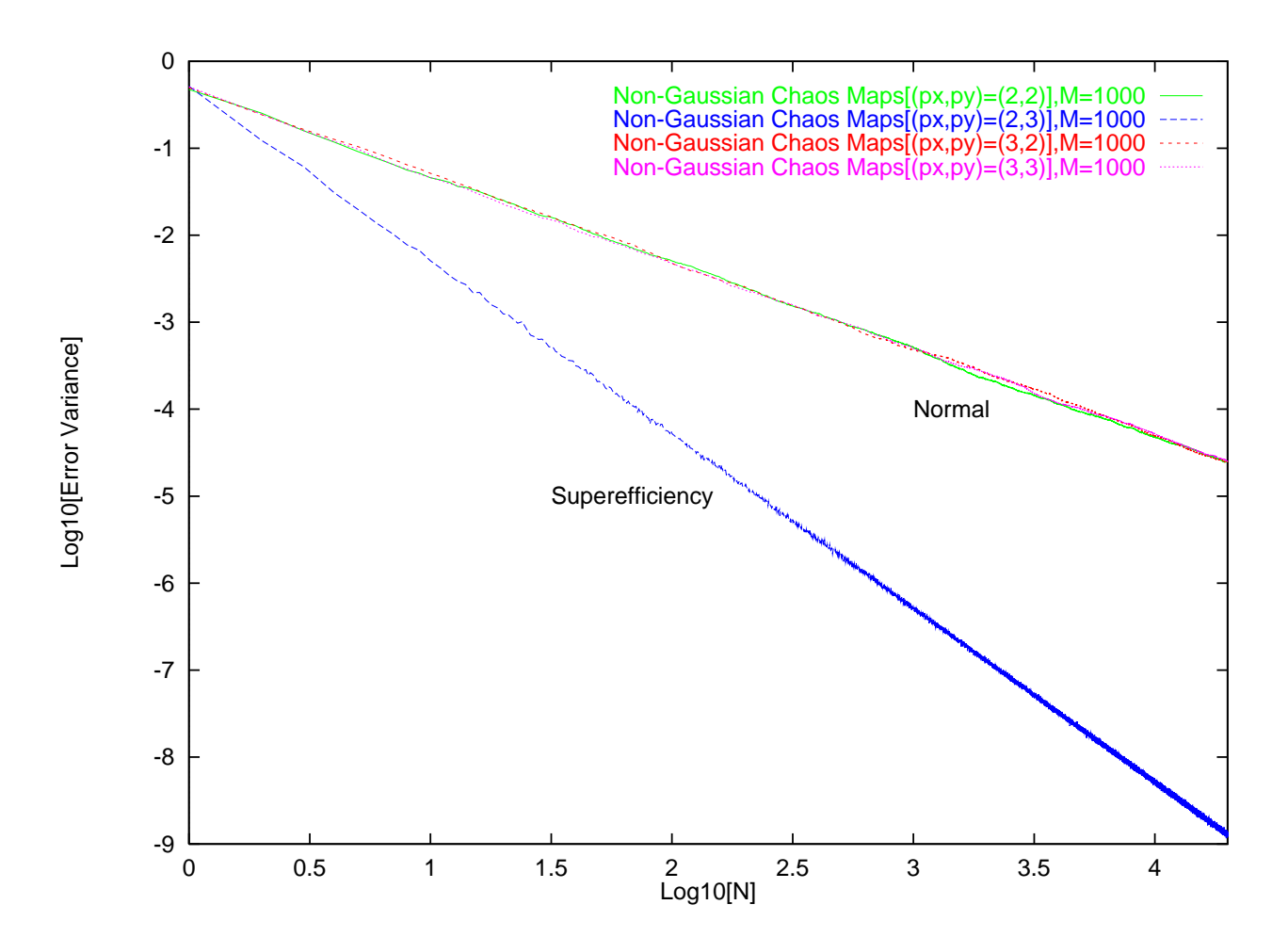


Fig. 8 Ken Umeno

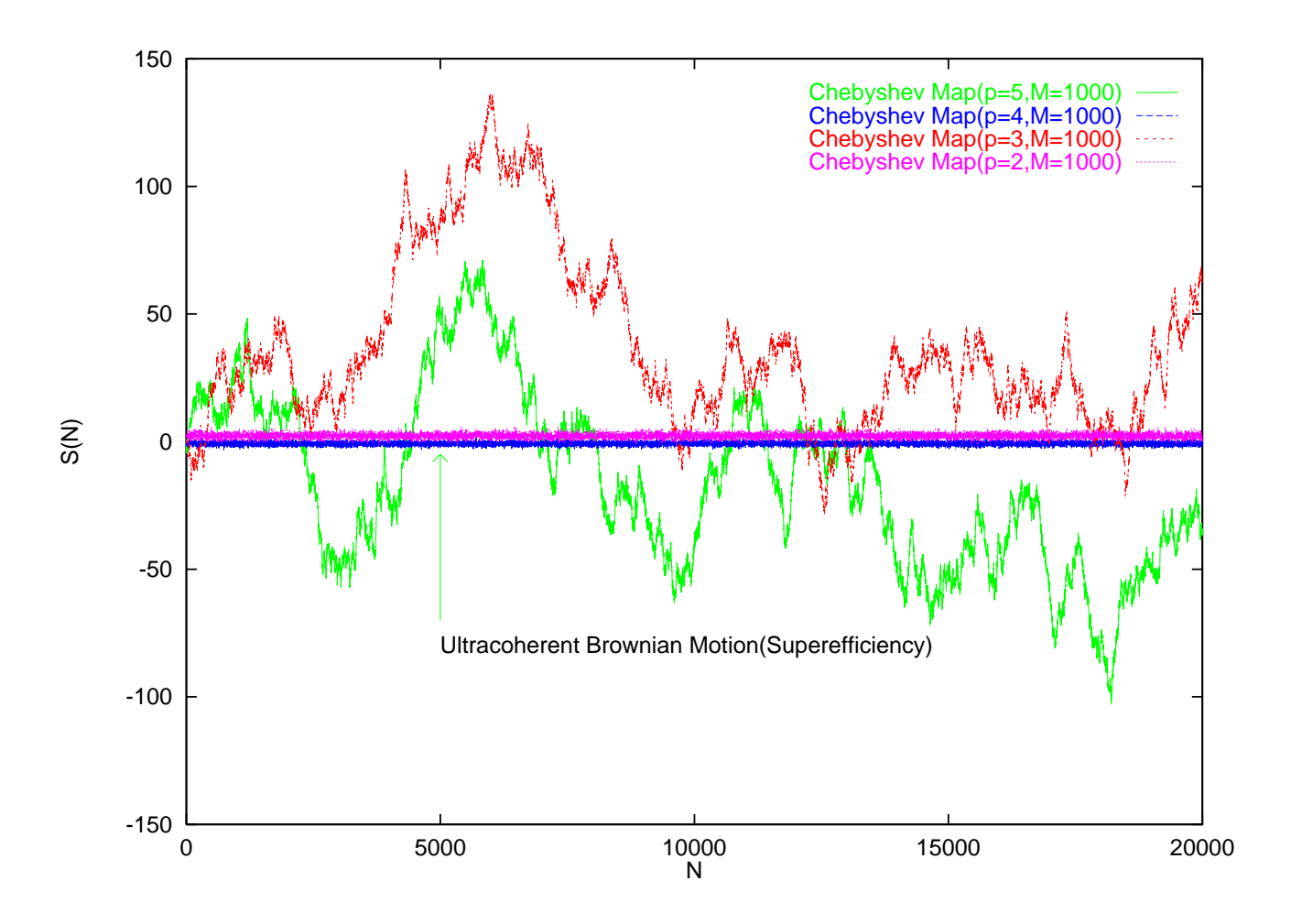


Fig. 9(a) Ken Umeno

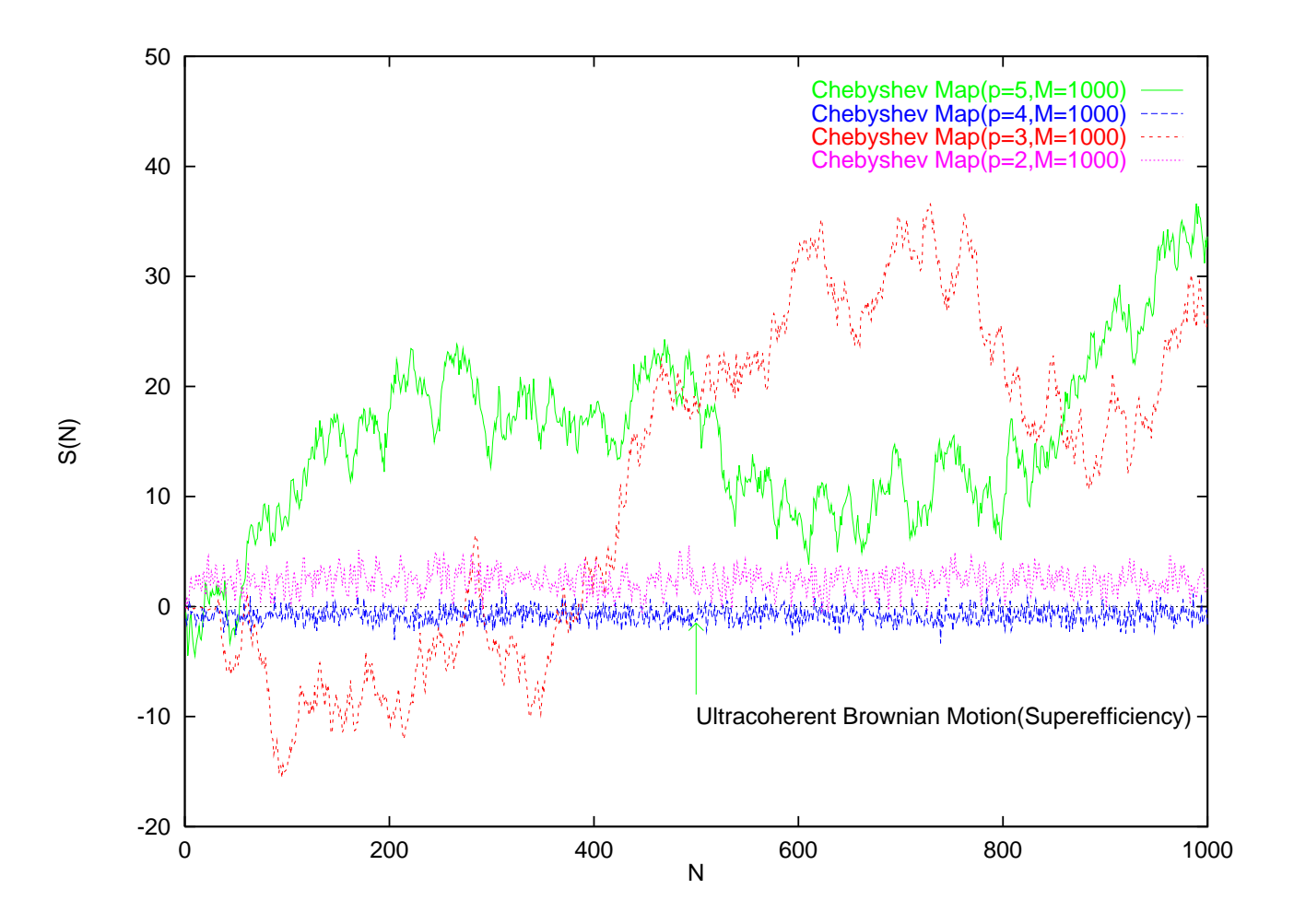


Fig. 9(b) Ken Umeno